AIMS Mathematics, 10(9): 20642–20669.
DOI: 10.3934/math.2025922
Received: 14 July 2025
Revised: 25 August 2025
Accepted: 29 August 2025
Published: 09 September 2025

https://www.aimspress.com/journal/Math

Research article

Global properties of a delayed model for the dynamics of lumpy skin disease with vaccination efficacy

Nada A. Almuallem*

Department of Mathematics and Statistics, Faculty of Science, University of Jeddah, P.O. Box 80327, Jeddah 21589, Saudi Arabia

* **Correspondence:** Email: naalmouallim@uj.edu.sa.

Abstract: Lumpy skin disease (LSD) is a viral infection in cattle caused by the lumpy skin disease virus (LSDV). The purpose of this study was to examine the qualitative dynamics of the LSD model, including vaccine efficacy and different types of discrete time delays. The model considers LSD transmission in both susceptible and vaccinated populations. Local and global stability analyses have been conducted. A Lyapunov functional was developed, and LaSalle's invariance principle was utilized to demonstrate the global asymptotic stability of the model's equilibria. We have calculated the basic reproduction number R_0. The LSD-free equilibrium is globally asymptotically stable (GAS) when $R_0 \leq 1$, whereas the LSD-endemic equilibrium is GAS when $R_0 > 1$. The theoretical results have been confirmed through numerical simulations. The results have indicated that utilizing a combination of time delays is more effective in eradicating the LSD virus outbreak. From a biological perspective, the delay functions similarly to antiviral vaccines and treatments in mitigating the LSD outbreak. Furthermore, even when the vaccine efficacy vanishes, an extended incubation period and increased delays before infection with LSD significantly restrict viral transmission and inhibit the spread of the virus. Moreover, the results indicate that even with a high level of vaccine efficacy, the elimination of the disease from populations is unlikely without the implementation of supplementary mitigation strategies.

Keywords: LSD mathematical model; global stability; time delays; vaccine efficacy; numerical simulations
Mathematics Subject Classification: 34K20, 92D30, 37N25, 93C10

1. Introduction

Lumpy skin disease (LSD) is a highly transmissible viral condition in cattle, induced by the lumpy skin disease virus (LSDV), which belongs to the *Capripoxvirus* genus. From an economic perspective,

LSD presents a significant threat to nations reliant on cattle, particularly in emerging African and Asian countries [1]. The disease causes serious financial losses due to a drastic decline in milk production, impaired skin quality, chronic weakness, obesity, pregnancy loss, and mortality. It is also classified as a disease that must be reported, and in countries where it is endemic, it imposes significant limitations on international trade [2]. It was first recognized in Zambia in 1929. It spread to Zimbabwe and South Africa, resulting in a significant outbreak in 1949 that impacted around 8 million cattle. From 1950 to 1980, the disease proliferated throughout Africa, affecting nations including Kenya, Somalia, and Ethiopia. LSD arrived in Israel in 1989 and has subsequently proliferated throughout the Middle East, Europe, and West Asia, with significant outbreaks occurring in Greece, Georgia, and Russia between 2018 and 2019. In July 2019, LSD appeared in Bangladesh, impacting around 0.5 million cattle, and is now expanding quickly across India and Pakistan [1, 2].

LSD occurs through mechanical vectors, including biting flies and mosquitoes, and via direct contact with infected cattle or contaminated water. Environmental variables such as temperature and humidity greatly affect vector population dynamics, rendering LSD seasonal in numerous places [3]. The interval between inoculation and the initial detection of generalized clinical indications varies from 7 to 14 days in experimentally infected cattle, regardless of the infection source, and from 2 to 5 weeks in natural cases [2]. While there is no cure for lumpy skin disease, controlling it requires a comprehensive strategy that integrates vaccination, biosecurity measures, and vector control methods. The biosecurity protocols, which include the immediate isolation of infected animals, limitations on animal movement, cleaning of affected facilities, and proper disposal of deceased animals, are crucial for limiting transmission within and among herds. Moreover, vector control is vital, given that the virus is mainly transmitted by biting insects; control strategies involve the use of pesticides, environmental management to eradicate breeding places, and improved animal housing. Incorporating these control strategies is essential for managing diseases efficiently and preventing their global spread [2, 4].

Mathematical models for epidemic diseases play a crucial role in the area of epidemiology. Various epidemic models are being created and used to study and manage many diseases, including those that impact humans [5–7] as well as diseases that affect animals and plants [8–10]. Furthermore, some ordinary differential equation (ODE)–based epidemiological models that integrate vaccination have demonstrated the ability to generate complex dynamic patterns, varying from regular oscillations to chaotic behavior [11, 12]. In [13], researchers have also studied the role of cattle movement networks in disease spread. Analytical studies have established rigorous conditions for the local and global stability of equilibria in epidemiological systems, providing a theoretical foundation for the design of effective control measures [5, 14]. To our knowledge, we found insufficient research regarding the transmission dynamics and optimal control of LSD. For instance, a statistical approach was developed for the LSD virus that identifies several transmission methods in [15]. Authors in [16] investigated LSD infection in Africa, Asia, and Europe, using statistical methods to analyze the results. In [17], an SVEIR compartmental model was designed incorporating vaccination as a control measure. Gunaseelan et al. [18] employed Caputo–Fabrizio fractional-order derivatives to improve model accuracy for LSD. A new LSD model representing cows, flies, and temperature dependency was investigated in [19]. The authors in [20] formulated a novel mathematical model to examine the dynamics of lumpy skin disease in cattle, integrating essential epidemiological elements and an improved parameterization to facilitate comprehension and management of disease outbreaks. In [21],

the study showed that climate variations influence vector abundance and activity, resulting in significant seasonality in LSD epidemics. A small number of recent LSD mathematical models proposed and studied the dynamics of LSD and their controls, see [22–24] and the references therein.

Time delays are prevalent and significant in the modeling of epidemic diseases, since they explain observed oscillations and represent biological reality, including the time before symptoms appear and the period before people are affected by social interactions [25, 26]. In the epidemiology of LSD, biological and control-related delays significantly influence the dynamics of outbreaks. These delays arise from multiple phases in the transmission cycle; for example, the incubation period: following initial exposure to the LSD virus, infected cattle experience a latent period of 7 to 35 days prior to the onset of clinical signs or sickness. In this phase, cattle belong to the exposed class and are not yet facilitating additional transmission. Disregarding this delay in models may lead to an underestimate of the rate of epidemic transmission. Moreover, many factors impact the phase before the onset of LSD infection, such as limited social connection, quarantine, limitations on travel, extended vacations, hospitalization, variations in the climate, and isolation, whether related to government-mandated disease prevention measures or voluntary decisions by individuals [2].

All of the aforementioned LSD research did not account for realistic elements, such as biological delays. Moreover, vaccination is crucial in the modeling of epidemic dynamics. Experimental research [27] has shown that three to four weeks after getting the LSD vaccine, both vaccinated and unvaccinated cattle can still get infected with a highly contagious LSDV strain. Compared to unvaccinated cattle, vaccinated cattle exhibit reduced clinical severity and minimal visible signs of disease [27]. The limited efficacy of immunization derives from the utilization of an inadequate vaccine. Some mathematical epidemiological studies, e.g., tuberculosis [28], proposed post-vaccination, susceptible individuals receive partial protection against infection. Consequently, the author suggested that vaccinated individuals may become infected, at a reduced rate compared to susceptible individuals, following substantial exposure to an actively diseased person. In the context of LSD mathematical models, there is no study that proposed this assumption. To this end, the current model addresses these shortcomings, stemming from a disregard for vaccine efficacy and delays, by adding three types of time delays to better represent how the disease progresses and by including vaccine efficacy as a changing factor that affects how the disease spreads. These improvements offer a more realistic and adaptable framework for assessing control methods and forecasting disease behavior under different epidemiological situations. In this study, we develop a mathematical model mentioned in [17], which only looked at the ODE model and did not take into account how time delays affect the infection. Moreover, in [17], the author did not consider that vaccinated cattle can become infected again at a lower rate depending on the efficiency of the vaccine, which reduces the force of infection transmission of such vaccinated cattle, so the rate of transmission of vaccinated cattle is related to the infection transmission of susceptible cattle, and it is always less than or equal to this rate. The overall population is categorized into five compartments: susceptible LSD cattle, vaccinated LSD cattle, exposed LSD cattle, active LSD cattle, and recovered LSD cattle. The model includes three types of discrete-time delays to consider the time gaps between how susceptible and vaccinated cattle interact with actively infected cattle, along with the incubation period. The model also takes into consideration the vaccine's efficacy.

The structure of the work is as follows: Section 2 indicates the characterization of a delayed-LSD mathematical model. We also conduct an analytical investigation of the model's equilibria and their

local and global stability. Furthermore, through sensitivity analysis, we will identify the model parameters most sensitive to the reproduction number, which may facilitate more effective prevention of the disease. In Section 3, we show numerical findings for the baseline dynamics of this model, as well as the dynamics when varying the three types of time delays and vaccine efficacy. We conclude with a discussion in Section 4.

2. Delayed-LSD model

To examine the role of time delays and vaccination efficacy on the dynamics of LSD, we modify the mathematical model introduced in [17] by considering the presence of three types of time delays [2,26] and vaccine efficacy [28]. Thus, we focus on the following interactions between five compartments: the number of susceptible LSD cattle ($\mathcal{S}$), the number of vaccinated LSD cattle ($\mathcal{V}$), the number of exposed LSD cattle ($\mathcal{E}$), the number of active LSD cattle ($\mathcal{A}$), and the number of recovered LSD cattle ($\mathcal{R}$). The time development of these variables is illustrated by the subsequent equations:

$$\dot{\mathcal{S}}(t) = \lambda - \beta_s \mathcal{S}(t)\mathcal{A}(t) - (\gamma + m)\mathcal{S}(t), \tag{2.1a}$$

$$\dot{\mathcal{V}}(t) = \gamma \mathcal{S}(t) - \beta_v \mathcal{V}(t)\mathcal{A}(t) - (\omega + m)\mathcal{V}(t), \tag{2.1b}$$

$$\dot{\mathcal{E}}(t) = e^{-m\xi_1}\beta_s \mathcal{S}(t-\xi_1)\mathcal{A}(t-\xi_1) + e^{-m\xi_2}\beta_v \mathcal{V}(t-\xi_2)\mathcal{A}(t-\xi_2) - (p+m)\mathcal{E}(t), \tag{2.1c}$$

$$\dot{\mathcal{A}}(t) = e^{-m\xi_3} p\mathcal{E}(t-\xi_3) - (\delta + \sigma + m)\mathcal{A}(t), \tag{2.1d}$$

$$\dot{\mathcal{R}}(t) = \omega \mathcal{V}(t) + \delta \mathcal{A}(t) - m\mathcal{R}(t). \tag{2.1e}$$

Equations (2.1a)–(2.1e) describe the next mechanisms of biology, which are illustrated in Figure 1. For further clarification, refer to Tables 1 and 2, which provide descriptions of the model's variables and parameters:

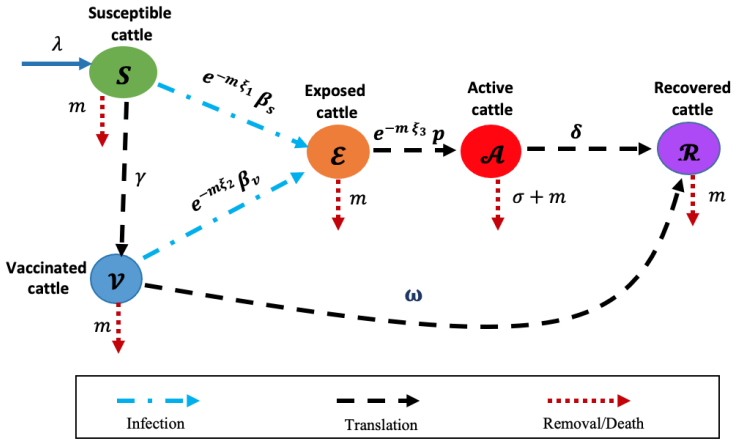

Figure 1. The flow diagram of the delayed-LSD model (2.1). λ and γ are the birth and vaccination rates of the susceptible cattle, respectively. β_s and β_v are the infection rates of susceptible cattle and vaccinated cattle, respectively. ω is the rate at which vaccinated cattle are recovering, p is the translation rate from $\mathcal{E}$ to $\mathcal{A}$, δ is the recovery rate of actively infected cattle, σ is the infection death rate, and ξ_1 and ξ_2 are the delays in the exposure to infection for $\mathcal{S}$ and $\mathcal{V}$, respectively. ξ_3 is the delay in the onset of LSD symptoms following an infection.

Table 1. Explanation of the model's variables.

Variable	Description
$\mathcal{S}$	Susceptible LSD cattle
$\mathcal{V}$	Vaccinated LSD cattle
$\mathcal{E}$	Exposed LSD cattle
$\mathcal{A}$	Active LSD cattle
$\mathcal{R}$	Recovered LSD cattle

Table 2. Parameter descriptions.

Param.	Description	Value	Unit	Ref.
λ	Birth rate	4	Individuals day^{-1}	[17]
m	Natural death rate	0.2	day^{-1}	[17]
β_s	Infection rate of susceptible cattle	0.39	(Individuals day)$^{-1}$	[17]
γ	Vaccination rate of susceptible cattle	0.3	day^{-1}	[17]
ω	Rate at which vaccinated cattle are recovering	0.1	$^{-1}$	[17]
p	Translation rate from $\mathcal{E}$ to $\mathcal{A}$	0.08/0.59	day^{-1}	[2]
δ	Recovery rate of actively infected cattle	0.055	day^{-1}	[2]
σ	Infection death rate	0.3	day^{-1}	[17]
κ_v	Vaccine efficacy	[0 − 1]0.5	-	[28]
ξ_1	Delay in the exposure to infection for $\mathcal{S}$	3 − 14(8)	days	[26]
ξ_2	Delay in the exposure to infection for V	3 − 14(8)	days	[26]
ξ_3	Delay in the onset of LSD symptoms following an infection	7 − 35(21)	days	[2]

2.1. Initial conditions

The initial conditions for model (2.1) are expressed as

$$\begin{aligned} &\mathcal{S}(\theta) = \Phi_1(\theta),\ \mathcal{V}(\theta) = \Phi_2(\theta),\ \mathcal{E}(\theta) = \Phi_3(\theta),\\ &\mathcal{A}(\theta) = \Phi_4(\theta),\ \mathcal{R}(\theta) = \Phi_5(\theta),\\ &\Phi_j(\theta) \geq 0,\ \theta \in [-\Xi, 0],\\ &\Phi_j(\theta)) \in \mathbb{C}([-\Xi, 0], \mathbb{R}^5_{\geq 0}), \quad j = 1, 2, ...5, \end{aligned} \tag{2.2}$$

where $\Xi = \max\{\tau_2, \tau_2, \tau_3\}$ and $\mathbb{C}$ denotes the Banach space of continuous functions defined on the interval $[-\Xi, 0]$ into $\mathbb{R}^5_{\geq 0}$. According to the fundamental theory of delay differential equations [29], model (2.1) holds a unique solution that meets the initial conditions (2.2) for $t > 0$.

- The susceptible LSD cattle ($\mathcal{S}$) (see Eq (2.1a)) are incorporated into the cattle population at a rate of λ. A constant input for such a form is frequently examined in LSD disease models [30]. We suggest that the proportion of new infections arising from interactions between susceptible and active LSD-infected individuals is $\beta_s \mathcal{S}\mathcal{A}$. The parameter β_s represents the level of infection or the rate of transmission. The bilinear rate, defined as a constant LSD infection rate per infected and susceptible individual, is frequently employed in deterministic compartmental

modeling [17, 30, 31]. Post-vaccination, vulnerable LSD cattle receive partial protection against LSD infection, hence boosting the vaccinated population at a rate of γ [17, 31]. This denotes the carrying out of the immunization initiative that protects livestock from LSD infection.

- The vaccinated LSD cattle ($\mathcal{V}$) in Eq (2.1b) can still become infected with LSD because the vaccine is not very effective. This means that vaccinated individuals can catch the disease from an infected one at a lower rate of $(1 - \kappa_v)$. The infection rate for vaccinated cattle is shown as $\beta_v \mathcal{V}\mathcal{A}$, where $\beta_v = (1 - \kappa_v)\beta_s$, which is usually lower than the infection rate for unvaccinated cattle, β_s [28]. Vaccinated cattle are recovering at a rate of ω [17, 31].
- The exposed LSD cattle ($\mathcal{E}$) in Eq (2.1c) are likely introduced to the LSD virus and may not yet exhibit symptoms. The exposed cattle will begin to exhibit symptoms of LSD, leading to an increase in the active LSD population at the rate of p. Moreover, the parameters $\xi_1 > 0$ and $\xi_2 > 0$ represent the period preceding the infection's transmission between the susceptible and vaccinated cattle with the active cattle, respectively, until they become exposed (i.e., infected but not yet active cattle). These time delays are, for example, because of the limited social interaction, either caused by government-mandated disease control measures or voluntary decisions made by humans. The factors $e^{-m\xi_1}$ and $e^{-m\xi_2}$ [32] represent the reduction of susceptible and vaccinated cattle (or the survival rate) during the times $[t - \xi_1, t]$ and $[t - \xi_2, t]$, respectively [26].
- The recovering cattle ($\mathcal{R}$), as referenced in Eq (2.1e), and all other populations exhibit a natural death rate of m. We have already defined all other terms previously (for more details about the delayed-LSD model (2.1), see Tables 1 and 2).

3. Mathematical analysis of the delayed-LSD model

3.1. Non-negativity and boundedness

In this section, we demonstrate the positivity and boundedness for the solutions to model (2.1) given initial conditions (2.2).

Proposition 1. *Let $(\mathcal{S}(t), \mathcal{V}(t), \mathcal{E}(t), \mathcal{A}(t), \mathcal{R}(t))$ be any solution of model (2.1) which satisfies the initial conditions (2.2), and then $\mathcal{S}(t), \mathcal{V}(t), \mathcal{E}(t), \mathcal{A}(t)$ and $\mathcal{R}(t)$ are all non-negative for $t \geq 0$ and ultimately bounded.*

Proof. In the beginning, we shall express model (2.1) in matrix notation $\dot{g}(t) = \mathcal{K}(g(t))$, where $g = (\mathcal{S}, \mathcal{V}, \mathcal{E}, \mathcal{A}, \mathcal{R})^T, \mathcal{K} = (\mathcal{K}_1, \mathcal{K}_2, \mathcal{K}_3, \mathcal{K}_4, \mathcal{K}_5)^T$, and

$$\mathcal{K}(g(t)) = \begin{pmatrix} \mathcal{K}_1(g(t)) \\ \mathcal{K}_2(g(t)) \\ \mathcal{K}_3(g(t)) \\ \mathcal{K}_4(g(t)) \\ \mathcal{K}_5(g(t)) \end{pmatrix}, \tag{3.1}$$

$$\mathcal{K} = \begin{pmatrix} \lambda - \beta_s \mathcal{S}(t)\mathcal{A}(t) - (\gamma + m)\mathcal{S}(t) \\ \gamma \mathcal{S}(t) - \beta_v \mathcal{V}(t)\mathcal{A}(t) - (\omega + m)\mathcal{V}(t) \\ e^{-m\xi_1}\beta_s \mathcal{S}(t - \xi_1)\mathcal{A}(t - \xi_1) + e^{-m\xi_2}\beta_v \mathcal{V}(t - \xi_2)\mathcal{A}(t - \xi_2) - (p + m)\mathcal{E}(t) \\ e^{-m\xi_3} p\mathcal{E}(t - \xi_3) - (\delta + \sigma + m)\mathcal{A}(t) \\ \omega \mathcal{V}(t) + \delta \mathcal{A}(t) - m\mathcal{R}(t) \end{pmatrix}. \tag{3.2}$$

We have

$$\mathcal{K}_j(g(t))|_{g(t)\in\mathbb{R}^5_{>0}} \geq 0, \quad j = 1, ..., 5. \tag{3.3}$$

Utilizing Lemma 2 in [33], the solutions of model (2.1) with the initial conditions (2.2) satisfy $g(t) \in \mathbb{R}^5_{\geq 0}$ for all $t \geq 0$.

Following that, we verify the boundedness of the solutions. Using Eq (2.1a), we get $\mathcal{S}(t) \leq \lambda - (\gamma + m)\mathcal{S}(t)$, which implies that $\limsup_{t\to\infty} \mathcal{S}(t) \leq \frac{\lambda}{\gamma+m} = L_1$. From Eq (2.1b), we have $\dot{\mathcal{V}}(t) \leq \gamma\mathcal{S} - (\omega + m)\mathcal{V}$, and therefore

$$\limsup_{t\to\infty} \mathcal{V}(t) \leq \frac{\lambda\gamma}{(\gamma + m)(\omega + m)} = L_2.$$

Let $\mathcal{T}_1(t) = e^{-m\xi_1}\mathcal{S}(t - \xi_1) + e^{-m\xi_2}\mathcal{V}(t - \xi_2) + \mathcal{E}(t)$, and then

$$\begin{aligned}\dot{\mathcal{T}}_1(t) &= e^{-m\xi_1}\dot{\mathcal{S}}(t - \xi_1) + e^{-m\xi_2}\dot{\mathcal{V}}(t - \xi_2) + \dot{\mathcal{E}}(t)\\ &\leq \lambda e^{-m} + \gamma e^{-n_2}L_1 - \pi\mathcal{T}(t) \leq \lambda + \gamma L_1 - \pi\mathcal{T}(t),\end{aligned}$$

where $\pi = \min\{(\gamma + m), (\omega + m), (\delta + \sigma + m)\}$. Hence, $\limsup_{t\to\infty} \mathcal{T}(t) \leq L_3$, where $L_3 = \dfrac{\lambda + \gamma L_1}{\pi}$. Since $\mathcal{S}(t)$, $\mathcal{V}(t)$, and $\mathcal{E}(t)$ are all non-negative, hence $\limsup_{t\to\infty} \mathcal{E}(t) \leq L_3$ for all $t \geq 0$.

To prove the non-negativity for $\mathcal{A}(t)$ and $\mathcal{R}(t)$, we assume that $\mathcal{T}_2(t) = \mathcal{A}(t) + \mathcal{R}(t)$, and then

$$\begin{aligned}\dot{\mathcal{T}}_2(t) &= \dot{\mathcal{A}}(t) + \dot{\mathcal{R}}(t)\\ &\leq \omega L_2 + pe^{-m\xi_3}L_3 - m\mathcal{T}_2(t) \leq \omega L_2 + pL_3 - m\mathcal{T}_2(t).\end{aligned}$$

Therefore, $\limsup_{t\to\infty} \mathcal{T}_2(t) \leq L_4$, where $L_4 = \dfrac{\omega L_2 + pL_3}{m}$. Since $\mathcal{A}(t)$ and $\mathcal{R}(t)$ are all non-negative, then, $\limsup_{t\to\infty} \mathcal{A}(t) \leq L_4$ and $\limsup_{t\to\infty} \mathcal{R}(t) \leq L_4$ for all $t \geq 0$. □

3.2. Equilibria and basic reproduction ratio

In this section, we compute the equilibria of model (2.1) and establish the basic reproduction ratio.

Proposition 2. *For model (2.1), there exists a basic reproduction number* $\mathsf{R}_0 > 0$ *such that*

(i) There exists a unique equilibrium point $\mathcal{D}^0$*, when* $\mathsf{R}_0 \leq 1$*, and*
(ii) There exist two equilibria, $\mathcal{D}^0$ *and* $\mathcal{D}^*$*, when* $\mathsf{R}_0 > 1$.

Proof. (i) The equilibrium points of model (2.1) meet the following conditions:

$$0 = \lambda - \beta_s\mathcal{S}\mathcal{A} - (\gamma + m)\mathcal{S}, \tag{3.4a}$$
$$0 = \gamma\mathcal{S} - \beta_v\mathcal{V}\mathcal{A} - (\omega + m)\mathcal{V}, \tag{3.4b}$$
$$0 = e^{-m\xi_1}\beta_s\mathcal{S}\mathcal{A} + e^{-m\xi_2}\beta_v\mathcal{V}\mathcal{A} - (p + m)\mathcal{E}, \tag{3.4c}$$
$$0 = e^{-m\xi_3}p\mathcal{E} - (\delta + \sigma + m)\mathcal{A}, \tag{3.4d}$$
$$0 = \omega\mathcal{V} + \delta\mathcal{A} - m\mathcal{R}. \tag{3.4e}$$

From Eqs (3.4a)–(3.4e), it is straightforward to demonstrate that when there is no LSD infection (i.e., $\mathcal{A} = 0$), model (1) possesses the free lumpy skin disease equilibrium point (LSD-free) $\mathcal{D}^0 = (\mathcal{S}^0, \mathcal{V}^0, \mathcal{E}^0, \mathcal{A}^0, \mathcal{R}^0) = (\frac{\lambda}{(\gamma+m)}, \frac{\lambda\gamma}{(\gamma+m)(\omega+m)}, 0, 0, \frac{\lambda\gamma\omega}{(\gamma+m)(\omega+m)m})$.

The basic reproduction number, represented as R_0, is a vital measure for assessing disease spread among a population. This parameter indicates the potential for the LSD to either become extinct or last within the population. Here, we obtain the formulation of the basic reproduction number by following the method outlined in [34]. According to the infected classes in model (2.1), arranged by $\mathcal{E}$ and $\mathcal{A}$, the non-linear terms corresponding to the new infection $\mathcal{X}$ and the outflow $\mathcal{G}$ are represented by the subsequent two matrices:

$$\mathcal{X} = \begin{pmatrix} e^{-m\xi_1}\beta_s\mathcal{S}\mathcal{A} + e^{-m\xi_2}\beta_v\mathcal{V}\mathcal{A} \\ 0 \end{pmatrix}, \quad \mathcal{G} = \begin{pmatrix} (p+m)\mathcal{E} \\ -e^{-m\xi_3}p\mathcal{E} + (\delta+\sigma+m)\mathcal{A} \end{pmatrix}. \tag{3.5}$$

The derivatives of $\mathcal{X}$ and $\mathcal{G}$ at the LSD-free equilibrium point $\mathcal{D}^0$ are provided by

$$\bar{\mathcal{X}} = \begin{pmatrix} 0 & e^{-m\xi_1}\beta_s\mathcal{S}^0 + e^{-m\xi_2}\beta_v\mathcal{V}^0 \\ 0 & 0 \end{pmatrix}, \quad \bar{\mathcal{G}} = \begin{pmatrix} p+m & 0 \\ -e^{-m\xi_3}p & \delta+\sigma+m \end{pmatrix}. \tag{3.6}$$

Therefore, R_0 can be obtained by using $\rho(\bar{\mathcal{X}}\bar{\mathcal{G}}^{-1})$, where $\rho(Y)$ is a spectral radius of matrix Y. Then, we get

$$\mathsf{R}_0 = \frac{[e^{-m\xi_1}\beta_s(\omega+m) + e^{-m\xi_2}\beta_v\gamma]\lambda e^{-m\xi_3}p}{(\gamma+m)(\omega+m)(p+m)(\delta+\sigma+m)}. \tag{3.7}$$

(ii) To identify the endemic equilibrium point for the delayed-LSD model (LSD-endemic) $\mathcal{D}^*$, together with $\mathcal{D}^0$, let $\mathcal{D}^* = (\mathcal{S}^*, \mathcal{V}^*, \mathcal{E}^*, \mathcal{A}^*, \mathcal{R}^*)$ be any equilibrium point of model (2.1) which satisfies the Eqs (3.4a)–(3.4e):

By solving Eqs (3.4b)–(3.4e), we derive the following formulas for $\mathcal{S}^*, \mathcal{V}^*, \mathcal{A}^*$, and $\mathcal{R}^*$ as follows:

$$\begin{aligned}
\mathcal{S}^* &= \frac{d_3d_4(e^{-m\xi_3}\beta_v p\mathcal{E}^* + d_2d_4)}{pe^{-m\xi_3}(e^{-m\xi_1}e^{-n_3\xi_3}p\beta_s\beta_v\mathcal{E}^* + d_2d_4e^{-m\xi_1}\beta_s + d_4\beta_v\gamma e^{-m\xi_2})}, \\
\mathcal{V}^* &= \frac{d_3d_4^2\gamma}{pe^{-m\xi_3}(p\beta_s\beta_v e^{-m\xi_1}e^{-m\xi_3}\mathcal{E}^* + d_2d_4e^{-m\xi_1}\beta_s + d_4e^{-m\xi_2}\beta_v\gamma)}, \quad \mathcal{A}^* = \frac{pe^{-m\xi_3}\mathcal{E}^*}{d_4}, \\
\mathcal{R}^* &= \frac{d_3d_4^3\omega\gamma + p^2\delta e^{-2m\xi_3}\mathcal{E}^*d_4(d_2e^{-m\xi_1}\beta_s + e^{-m\xi_2}\beta_v\gamma) + (\mathcal{E}^{*^2})p^3\beta_s\beta_v e^{-m\xi_1}\delta e^{-3m\xi_3})}{mpe^{-m\xi_3}d_4(\beta_s\beta_v pe^{-m\xi_1}e^{-m\xi_3}\mathcal{E}^* + d_2d_4\beta_s e^{-m\xi_1} + d_4e^{-m\xi_2}\beta_v\gamma)},
\end{aligned} \tag{3.8}$$

where $d_1 = (\gamma+m)$, $d_2 = (\omega+m)$, $d_3 = (p+m)$, and $d_4 = (\delta+\sigma+m)$. Substituting the values of $\mathcal{S}^*$ and $\mathcal{A}^*$ in Eq (3.4a) yields a quadratic equation in $\mathcal{E}^*$ as:

$$c_1\mathcal{E}^{*2} + c_2\mathcal{E}^* - c_3 = 0, \tag{3.9}$$

where

$$\begin{aligned}
c_1 &= d_3p^2e^{-2m\xi_3}\beta_s\beta_v, \\
c_2 &= (d_1d_3\beta_v + d_2d_3\beta_s)d_4pe^{-m\xi_3} - \beta_s\beta_v\lambda p^2e^{-m\xi_1}e^{-2m\xi_3}, \\
c_3 &= \lambda d_4pe^{-m\xi_3}(d_2e^{-m\xi_1}\beta_s + e^{-m\xi_2}\beta_v\gamma) - d_1d_2d_3d_4^2 = d_1d_2d_3d_4^2(\mathsf{R}_0 - 1).
\end{aligned}$$

The solutions of Eq (3.9) are given by:

$$\mathcal{E}^{*\pm} = \frac{-c_2 \pm \sqrt{c_2^2 + 4c_1c_3}}{2c_1}.$$

It is evident that $c_1 > 0$, and therefore if $c_3 > 0$ then $\mathcal{E}^{*+}$ and $\mathcal{E}^{*-} < 0$. Let $\mathcal{E}^* = \mathcal{E}^{*+}$, and then from Eq (3.8) we derive:

$$\mathcal{S}^* = \frac{d_3 d_4 (e^{-m\xi_3}\beta_v p\mathcal{E}^* + d_2 d_4)}{pe^{-m\xi_3}(e^{-m\xi_1}e^{-m\xi_3}p\beta_s\beta_v\mathcal{E}^* + d_2 d_4 e^{-m\xi_1}\beta_s + d_4\beta_v\gamma e^{-m\xi_2})} > 0,$$
$$\mathcal{V}^* = \frac{d_3 d_4^2\gamma}{pe^{-m\xi_3}(p\beta_s\beta_v e^{-m\xi_1}e^{-m\xi_3}\mathcal{E}^* + d_2 d_4 e^{-m\xi_1}\beta_s + d_4 e^{-m\xi_2}\beta_v\gamma)} > 0, \quad \mathcal{A}^* = \frac{pe^{-m\xi_3}\mathcal{E}^*}{d_4} > 0,$$
$$\mathcal{R}^* = \frac{d_3 d_4^3\omega\gamma + p^2\delta e^{-2m\xi_3}\mathcal{E}^* d_4(d_2 e^{-m\xi_1}\beta_s + e^{-m\xi_2}\beta_v\gamma) + \mathcal{E}^{*2}p^3\beta_s\beta_v e^{-m\xi_1}\delta e^{-3m\xi_3})}{mpe^{-m\xi_3}d_4(\beta_s\beta_v pe^{-m\xi_1}e^{-m\xi_3}\mathcal{E}^* + d_2 d_4\beta_s e^{-m\xi_1} + d_4 e^{-m\xi_2}\beta_v\gamma)} > 0. \tag{3.10}$$

Therefore, the LSD endemic equilibrium (LSD-endemic) $\mathcal{D}^* = (\mathcal{S}^*, \mathcal{V}^*, \mathcal{E}^*, \mathcal{A}^*, \mathcal{R}^*)$ exists when $c_3 > 0$ or $\mathsf{R}_0 > 1$. In this case where $\mathsf{R}_0 > 1$, the behavior of the system will be governed by the LSD-endemic equilibrium $\mathcal{D}^*$, indicating that the infection will persist in the cattle population continuously over a long time (the infection becoming endemic). □

3.3. Bifurcation analysis

This section examines the bifurcations demonstrated by the proposed model, highlighting the significance of certain parameters in shaping the system's dynamics as well as creating the conditions for transitions between equilibrium states, with an emphasis on transcritical bifurcations. A transcritical bifurcation emerges when $\mathsf{R}_0 = 1$. Subsequently, the LSD-free equilibrium (D^0) becomes unstable, leading to the emergence of a new endemic equilibrium (D^*), which indicates the continued existence of the disease. Moreover, at the bifurcation point $\mathsf{R}_0 = 1$ the Jacobian matrix analyzed at the LSD-free equilibrium (see, Section 3.4.1) possesses one eigenvalue of zero, whereas all other eigenvalues have negative real parts. This makes the equilibrium non-hyperbolic. As the bifurcation parameter crosses the threshold, this zero eigenvalue alters its sign, resulting in a stability exchange between the LSD-free and LSD-endemic equilibria. The eigenvalue switching verifies that the model experiences a forward transcritical bifurcation. For more details on types of bifurcation, see [35] and the references therein. Figure 2 illustrates the variation of the two distinct equilibrium points $\mathcal{D}^0$ and $\mathcal{D}^*$ as we modify three categories of delays: (a) delay in infection transmission between $\mathcal{S}$ and $\mathcal{A}$ (ξ_1), (b) delay in the incubation period of infected cattle that are not yet infectious (ξ_3), and (c) common delay (ξ_e) (without losing generality, we set $\xi_e = \xi_1 = \xi_2 = \xi_3$). We can see that an increase in ξ_1 above $\xi_1 = 9$ days, an increase of ξ_3 above $\xi_3 = 6.9$, or an increase in the common delay ξ_e above $\xi_e = 3.94$ causes the system to transition from an LSD-endemic state to an LSD-free state. The thresholds are designated as BP1, BP2, and BP3, represented in Figure 2 . Furthermore, it is evident that ξ_e stabilizes the system (driving the population to an LSD-free state) at a lower value than ξ_1 and ξ_3, as indicated by its lower bifurcation point (BP3). A smaller bifurcation threshold indicates that ξ_e is more effective in regulating disease dynamics. Applying multiple interventions or factors that impact the common delay, (ξ_e) would be more effective in eradicating LSD with reduced effort, cost, and resource allocation than those aimed at ξ_1 or ξ_3. To increase the delay ξ_e (i.e., increase ξ_1, ξ_2, and ξ_3), we may implement quarantine measures for newly introduced animals, decrease cattle density to minimize close contact, and adapt movement patterns (e.g., rotating feeding) to diminish mixing; these factors will increase ξ_1 and ξ_2. Furthermore, the increase in ξ_3 can be applied by using effective therapy or a vaccine to extend the LSD incubation period. Note that targeting some methods to

increase each delay separately requires more days to become rid of infection. In the next section, we will prove the stability of both equilibrium points, and we will show that when $\mathsf{R}_0 \leq 1$, the LSD-free equilibrium $\mathcal{D}^0$ is GAS, and when $\mathsf{R}_0 > 1$, the LSD-endemic equilibrium $\mathcal{D}^*$ is GAS, which confirms a forward transcritical bifurcation at $\mathsf{R}_0 = 1$ (see also Remark 1).

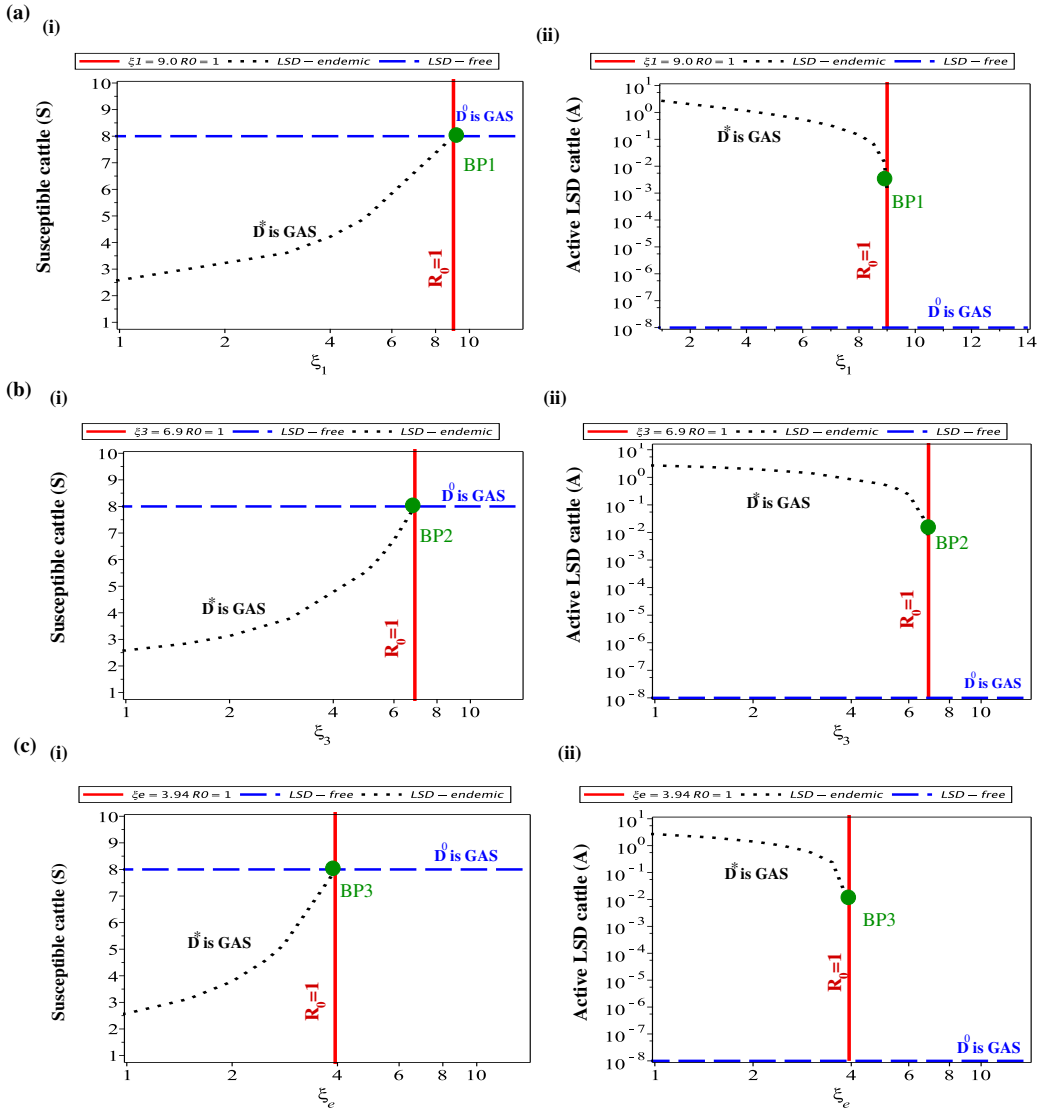

Figure 2. Bifurcation diagram for the two steady states calculated for the model (2.1), $\mathcal{D}^0$ and $\mathcal{D}^*$, as the time delays are varied: (a) delay of infection transmission between $\mathcal{S}$ and $\mathcal{A}$ (ξ_1), $\xi_1 \in [1, 14]$; (b) delay of incubation period of infected cattle that are not yet infectious (ξ_3), $\xi_3 \in [1, 14]$; (c) common delay ($\xi_e = \xi_1 = \xi_2 = \xi_3$), $\xi_e \in [1, 14]$. Sub-panel (i) shows $\mathcal{S}$ vs. time delay, while Sub-panel (ii) show $\mathcal{A}$ vs. time delay. "BP1" shows the bifurcation point where the $\mathcal{D}^*$ state bifurcates out of the $\mathcal{D}^0$ state as we decrease ξ_1 below $\xi_1 = 9.0$ (or $\mathsf{R}_0 = 1$), "BP2" demonstrates the bifurcation point where the $\mathcal{D}^*$ state bifurcates out of the $\mathcal{D}^0$ state as we decrease ξ_3 below $\xi_3 = 6.9$ (or $\mathsf{R}_0 = 1$), and "BP3" presents the bifurcation point where the $\mathcal{D}^*$ state bifurcates out of the LSD-free state as we decrease ξ_e below $\xi_e = 3.94$ (or $\mathsf{R}_0 = 1$).

3.4. Stability analysis

This section examines the local and global stability of the equilibria in the delayed-LSD model (2.1).

3.4.1. Local asymptotic stability

Theorem 1. *The LSD-free equilibrium point $\mathcal{D}^0$ is locally asymptotically stable (LAS), if $\mathsf{R}_0 < 1$, and is otherwise unstable.*

Proof. The linearization of the model (2.1) around the LSD-free equilibrium point $\mathcal{D}^0$ is represented by the Jacobian matrix:

$$\mathcal{J}_{(\mathcal{S}^0,\mathcal{V}^0,\mathcal{E}^0,\mathcal{A}^0,\mathcal{R}^0)} = \begin{bmatrix} -(\gamma+m) & 0 & 0 & -\frac{\lambda\beta_s}{m+\gamma} & 0 \\ \gamma & -(\omega+m) & 0 & -\frac{\gamma\beta_v\lambda}{(m+\gamma)(m+\omega)} & 0 \\ 0 & 0 & -(p+m) & \frac{\lambda e^{-m\xi_1}\beta_s}{m+\gamma} + \frac{e^{-m\xi_2}\gamma\beta_v\lambda}{(m+\gamma)(m+\omega)} & 0 \\ 0 & 0 & e^{-m\xi_3}p & -(m+\delta+\sigma) & 0 \\ 0 & \omega & 0 & \delta & -m \end{bmatrix}.$$

The aforementioned Jacobian matrix has three negative eigenvalues: $-(\gamma+m)$, $-(\omega+\mu)$, and $-m$. The rest of the eigenvalues can be obtained from the subsequent characteristic polynomial:

$$P(S) = S^2 + aS + b. \tag{3.11}$$

According to Routh-Hurwitz criteria, Eq (3.11) has negative real parts when

$$a = p + 2m + \delta + \sigma > 0$$

and

$$b = (p+m)(\delta+\sigma+m)\left(1 - \frac{[e^{-m\xi_1}\beta_s(m+\omega) + e^{-m\xi_2}\beta_v\gamma]\lambda p e^{-m\xi_3}}{(m+\omega)(m+\gamma)(p+m)(\delta+\sigma+m)}\right) \tag{3.12}$$

$$= (p+m)(\delta+\sigma+m)(1-\mathsf{R}_0) > 0. \tag{3.13}$$

Therefore the LSD-free $\mathcal{D}^0$ is LAS when $\mathcal{R}_0 < 1$, and is otherwise unstable. From a biological perspective, Theorem 1 indicates that lumpy skin disease can be eradicated from the community (when $\mathcal{R}_0 < 1$) if the initial population sizes in the model reside inside the basin of attraction of $\mathcal{E}^0$. To guarantee that elimination of LSD is unaffected by the initial population sizes, it is essential to demonstrate that $\mathcal{D}^0$ is globally asymptotically stable. This can be obtained below in Theorem 2. □

3.4.2. Global asymptotic stability

In this subsection, we examine the global stability of the two equilibria of model (2.1) utilizing the direct Lyapunov approach and LaSalle's invariance assumption. The next function will be applied throughout the paper. $Z : (0,\infty) \to [0,\infty)$ as:

$$Z(u) = u - 1 - \ln u. \tag{3.14}$$

Theorem 2. *The LSD-free equilibrium $\mathcal{D}^0$ for model (2.1) is globally asymptotically stable (GAS) if* $\mathsf{R}_0 \leq 1$.

Proof. We have the Lyapunov function

$$\mathfrak{V} = \Upsilon\Bigg[e^{-m\xi_1}\mathcal{S}^0 Z\left(\frac{\mathcal{S}}{\mathcal{S}^0}\right) + e^{-m\xi_2}\mathcal{V}^0 Z\left(\frac{\mathcal{V}}{\mathcal{V}^0}\right) + \mathcal{E} + e^{-m\xi_1}\beta_s \int_0^{\xi_1} \mathcal{S}(t-\theta)\mathcal{A}(t-\theta)d\theta$$
$$+ e^{-m\xi_2}\beta_v \int_0^{\xi_2} \mathcal{V}(t-\theta)\mathcal{A}(t-\theta)d\theta + (p+m)\int_0^{\xi_3} \mathcal{E}(t-\theta)d\theta\Bigg] + \frac{(p+m)}{(\omega+m)}\mathcal{A}, \tag{3.15}$$

where $\Upsilon = \frac{pe^{-m\xi_3}}{(\omega+m)}$. Along the trajectories of model (2.1), we calculate $\frac{d\mathfrak{V}_0}{dt}$ as:

$$\begin{aligned}
\frac{d\mathfrak{V}_0}{dt} &= \Upsilon\Bigg[e^{-m\xi_1}\left(1-\frac{\mathcal{S}^0}{\mathcal{S}}\right)(\lambda - \beta_s\mathcal{S}\mathcal{A} - (\gamma+m)\mathcal{S}) + e^{-m\xi_2}\left(1-\frac{\mathcal{V}^0}{\mathcal{V}}\right)(\gamma\mathcal{S} - \beta_v\mathcal{V}\mathcal{A} - (\omega+m)\mathcal{V}) \\
&\quad + e^{-m\xi_1}\beta_s\mathcal{S}(t-\xi_1)\mathcal{A}(t-\xi_1) + e^{-m\xi_2}\beta_v\mathcal{V}(t-\xi_2)\mathcal{A}(t-\xi_2) - (p+m)\mathcal{E} \\
&\quad + e^{-m\xi_1}(\beta_s\mathcal{S}\mathcal{A} - \beta_s\mathcal{S}(t-\xi_1)\mathcal{A}(t-\xi_1)) + e^{-m\xi_2}(\beta_V\mathcal{V}\mathcal{A} - \beta_s\mathcal{S}(t-\xi_2)\mathcal{A}(t-\xi_2)) \\
&\quad + (p+m)(\mathcal{E} - \mathcal{E}(t-\xi_3))\Bigg] + \frac{(p+m)}{(\omega+m)}(e^{-m\xi_3}p\mathcal{E}(t-\xi_3) - (\delta+\sigma+m)\mathcal{A}). \\
&= \Upsilon\left[(\gamma+m)e^{-m\xi_1}\left(1-\frac{\mathcal{S}^0}{\mathcal{S}}\right)(\mathcal{S}^0-\mathcal{S}) + (\omega+m)e^{-m\xi_2}\left(1-\frac{\mathcal{V}^0}{\mathcal{V}}\right)\left(\frac{\gamma\mathcal{S}}{(\omega+m)} - \mathcal{V}\right)\right] \\
&\quad + \left(\frac{pe^{-m\xi_3}}{(\omega+m)}e^{-m\xi_1}\beta_s\mathcal{S}^0 + \frac{pe^{-m\xi_3}}{(\omega+m)}e^{-m\xi_2}\beta_v\mathcal{V}^0 - \frac{(p+m)(\delta+\sigma+m)}{(\omega+m)}\right)\mathcal{A}.
\end{aligned} \tag{3.16}$$

Since $\mathcal{S}^0 \geq \mathcal{S}$, and after collecting the terms of Eq (3.16), we obtain

$$\frac{d\mathfrak{V}_0}{dt} \leq -\Upsilon e^{-m\xi_1}(\gamma+m)\frac{(\mathcal{S}-\mathcal{S}^0)^2}{S} - \Upsilon e^{-m\xi_2}(\omega+m)\frac{(\mathcal{V}-\mathcal{V}^0)^2}{V} + \frac{(p+m)(\delta+\sigma+m)}{(\omega+m)}(\mathcal{R}_0-1)\mathcal{A}. \tag{3.17}$$

Thus, if $\mathcal{R}_0 \leq 1$, then $\frac{d\mathfrak{V}_0}{dt} \leq 0$ for all $\mathcal{S}, \mathcal{V}, \mathcal{A} > 0$. Using Theorem 5.3.1 in [36], the model's solutions are limited to Γ, the largest invariant subset of $\left\{\frac{d\mathfrak{V}_0}{dt} = 0\right\}$. Given Eq (3.17) we get $\frac{d\mathfrak{V}_0}{dt} = 0$ if and only if $\mathcal{S} = \mathcal{S}^0$, $\mathcal{V} = \mathcal{V}^0$, and $\mathcal{A} = 0$. The set Γ is invariant, and for every element in Γ, it holds that $\mathcal{A} = 0$, and therefore $\dot{\mathcal{A}} = 0$. We can observe from model (2.1) as t approaches ∞ that we get

$$\mathcal{E} \to 0, \mathcal{R} \to \frac{\lambda\gamma\omega}{m(m+\gamma)(m+\omega)}. \tag{3.18}$$

Thus, $\frac{d\mathfrak{V}_0}{dt} = 0$ if and only if $\mathcal{S} = \mathcal{S}^0$, $\mathcal{V} = \mathcal{V}^0$, $\mathcal{A} = \mathcal{E} = 0$, and $\mathcal{R} = \frac{\lambda\gamma\omega}{m(m+\gamma)(m+\omega)}$. Utilizing LaSalle's invariance principle [37], the point $\mathcal{D}^0$ is GAS. □

Next, we examine the global stability of the endemic equilibrium of model (2.1). For complete mathematical tractability, we will focus just on a specific case: ($\kappa_v = 1$), indicating that the efficacy of the vaccine is 100%. Subsequently, model (2.1) becomes

$$\dot{\mathcal{S}}(t) = \lambda - \beta_s\mathcal{S}(t)\mathcal{A}(t) - (\gamma+m)\mathcal{S}(t),$$

$$\begin{aligned}
\dot{\mathcal{V}}(t) &= \gamma\mathcal{S}(t) - (\omega + m)\mathcal{V}(t),\\
\dot{\mathcal{E}}(t) &= e^{-m\xi_1}\beta_s\mathcal{S}(t-\xi_1)\mathcal{A}(t-\xi_1) - (p+m)\mathcal{E}(t),\\
\dot{\mathcal{A}}(t) &= e^{-m\xi_3}p\mathcal{E}(t-\xi_3) - (\delta + \sigma + m)\mathcal{A}(t),\\
\dot{\mathcal{R}}(t) &= \omega\mathcal{V}(t) + \delta\mathcal{A}(t) - m\mathcal{R}(t).
\end{aligned} \tag{3.19}$$

For model (3.19), the basic reproduction number is

$$\mathsf{R}_0 = \frac{e^{-m\xi_1}e^{-m\xi_3}\beta_s\lambda p}{(\gamma+m)(p+m)(\delta+\sigma+m)}.$$

When $\mathsf{R}_0 > 1$, then $\mathcal{D}^* > 0$, and model (3.19) has a positive equilibrium $\mathcal{D}^* = (\mathcal{S}^*, \mathcal{V}^*, \mathcal{E}^*, \mathcal{A}^*, \mathcal{R}^*)$, where

$$\begin{aligned}
\mathcal{S}^* &= \frac{d_3d_4}{pe^{-m\xi_3}e^{-m\xi_1}\beta_s} > 0,\\
\mathcal{V}^* &= \frac{d_3d_4\gamma}{pe^{-m\xi_3}e^{-m\xi_1}\beta_s d_2} > 0, \quad \mathcal{A}^* = \frac{d_1(\mathsf{R}_0-1)}{\beta_s} > 0,\\
\mathcal{R}^* &= \frac{d_1\delta p d_2 e^{-m\xi_1}e^{-m\xi_3}(\mathsf{R}_0-1) + d_3d_4\omega\gamma}{pe^{-m\xi_1}e^{-m\xi_3}\beta_s d_2 m} > 0,\\
\mathcal{E}^* &= \frac{d_4d_1}{pe^{-m\xi_3}\beta_s}(\mathsf{R}_0-1),
\end{aligned} \tag{3.20}$$

where $d_1 = (\gamma+m)$, $d_2 = (\omega+m)$, $d_3 = (p+m)$, and $d_4 = (\delta+\sigma+m)$.

Here, we examine the global stability of the LSD-endemic equilibrium $\mathcal{D}^*$ for model (3.19).

Theorem 3. *For model (3.19), the LSD-endemic equilibrium $\mathcal{D}^*$ is globally asymptotically stable (GAS), if $\mathsf{R}_0 > 1$.*

Proof. Consider the Lyapunov function $\mathfrak{V}_2$:

$$\begin{aligned}
\mathfrak{V}_2 = \Upsilon\Bigg[&\mathcal{S}^*Z\left(\frac{\mathcal{S}}{\mathcal{S}^*}\right) + \frac{1}{\mathsf{F}}\mathcal{E}^*Z\left(\frac{\mathcal{E}}{\mathcal{E}^*}\right) + \frac{1}{\mathsf{F}}\beta_s\mathcal{S}^*\mathcal{A}^*e^{-m\xi_1}\int_0^{\xi_1} Z\left(\frac{\mathcal{S}(t-\theta)\mathcal{A}(t-\theta)}{S^*A^*}\right)d\theta\\
&+ \frac{(\omega+m)\mathcal{E}^*}{\mathsf{FG}}e^{-m\xi_3}\int_0^{\xi_3} Z\left(\frac{\mathcal{E}(t-\theta)}{\mathcal{E}^*}\right)d\theta\Bigg] + \mathcal{A}^*Z\left(\frac{\mathcal{A}}{\mathcal{A}^*}\right),
\end{aligned}$$

where $\mathsf{F} = e^{-m\xi_1}$ and $\mathsf{G} = e^{-m\xi_3}$. Calculating $\frac{d\mathfrak{V}_2}{dt}$ along the solutions of model (3.19), we get

$$\begin{aligned}
\frac{d\mathfrak{V}_2}{dt} = \Upsilon\Bigg[&\left(1-\frac{\mathcal{S}^*}{\mathcal{S}}\right)(\lambda - \beta_s\mathcal{S}\mathcal{A} - (\gamma+m)\mathcal{S})\\
&+ \frac{1}{\mathsf{F}}\left(1-\frac{\mathcal{E}^*}{\mathcal{E}}\right)(e^{-m\xi_1}\beta_s\mathcal{S}(t-\xi_1)\mathcal{A}(t-\xi_1) - (p+m)\mathcal{E})\\
&+ \beta_s\mathcal{S}\mathcal{A} - \beta_s\mathcal{S}(t-\xi_1)\mathcal{A}(t-\xi_1) + \beta_s\mathcal{S}^*\mathcal{A}^*\ln\left(\frac{\mathcal{S}(t-\xi_1)\mathcal{A}(t-\xi_1)}{\mathcal{S}\mathcal{A}}\right)
\end{aligned}$$

$$+\frac{(\omega+m)e^{-m\xi_3}\mathcal{E}^*}{\mathsf{FG}}\left(\frac{\mathcal{E}}{\mathcal{E}^*}-\frac{\mathcal{E}(t-\xi_3)}{\mathcal{E}^*}+\ln\left(\frac{\mathcal{E}(t-\xi_3)}{\mathcal{E}}\right)\right)\Bigg]$$
$$+\left(1-\frac{\mathcal{A}^*}{\mathcal{A}}\right)\left(e^{-m\xi_3}p\mathcal{E}(t-\xi_3)-(\delta+\sigma+m)\mathcal{A}\right). \tag{3.21}$$

Collecting terms of Eq (3.21) we have

$$\frac{d\mathfrak{V}_2}{dt}=\Upsilon\Bigg[\left(1-\frac{\mathcal{S}^*}{\mathcal{S}}\right)(\lambda-(\gamma+m)\mathcal{S})+\beta_s\mathcal{S}^*\mathcal{A}+\frac{(\omega+m)}{F}\mathcal{E}^*+\frac{(\omega+m)(p+m)}{pFG}\mathcal{A}^*$$
$$-\frac{e^{-m\xi_1}\beta_s}{F}\frac{\mathcal{E}^*\mathcal{S}(t-\xi_1)\mathcal{A}(t-\xi_1)}{\mathcal{E}}-\frac{(\omega+m)e^{-m\xi_3}}{FG}\frac{\mathcal{A}^*\mathcal{E}(t-\xi_3)}{\mathcal{A}}$$
$$+\frac{e^{-m\xi_1}}{F}\beta_s\mathcal{S}^*\mathcal{A}^*\ln\left(\frac{S(t-\xi_1)A(t-\xi_1)}{\mathcal{S}\mathcal{A}}\right)+\frac{(\omega+m)e^{-m\xi_3}}{\mathsf{FG}}\mathcal{E}^*\ln\left(\frac{\mathcal{E}(t-\xi_3)}{\mathcal{E}}\right)\Bigg]-(p+m)\mathcal{A}.$$

The positive equilibrium $\mathcal{D}^*=(\mathcal{S}^*,\mathcal{V}^*,\mathcal{E}^*,\mathcal{A}^*,\mathcal{R}^*)$ holds for the following conditions.

$$\lambda=\beta_s\mathcal{S}^*\mathcal{A}^*+(\gamma+m)\mathcal{S}^*,\ (p+m)=\frac{e^{-m\xi_1}\beta_s\mathcal{S}^*\mathcal{A}^*}{\mathcal{E}^*},\ (\delta+\sigma+m)=\frac{e^{-m\xi_3}p\mathcal{E}^*}{\mathcal{A}^*}.$$

Then, we obtain

$$\frac{d\mathfrak{V}_2}{dt}=\Upsilon\Bigg[(\gamma+m)\left(1-\frac{\mathcal{S}^*}{\mathcal{S}}\right)(\mathcal{S}^*-\mathcal{S})+\beta_s\mathcal{S}^*\mathcal{A}^*\left(1-\frac{\mathcal{S}^*}{\mathcal{S}}\right)+2\beta_s\mathcal{S}^*\mathcal{A}^*$$
$$-\frac{e^{-m\xi_1}\beta_s\mathcal{S}^*\mathcal{A}^*}{F}\left(\frac{\mathcal{E}^*\mathcal{S}(t-\xi_1)\mathcal{A}(t-\xi_1)}{\mathcal{E}\mathcal{S}^*\mathcal{A}^*}\right)-\frac{e^{-m\xi_3}\beta_s\mathcal{S}^*\mathcal{A}^*}{G}\left(\frac{\mathcal{A}^*\mathcal{E}(t-\xi_3)}{\mathcal{A}\mathcal{E}^*}\right)$$
$$+\frac{e^{-m\xi_1}\beta_s\mathcal{S}^*\mathcal{A}^*}{F}\ln\left(\frac{\mathcal{S}(t-\xi_1)\mathcal{A}(t-\xi_1)}{\mathcal{S}\mathcal{A}}\right)+\frac{e^{-m\xi_3}\beta_s\mathcal{S}^*\mathcal{A}^*}{G}\ln\left(\frac{\mathcal{E}(t-\xi_3)}{\mathcal{E}}\right)\Bigg]. \tag{3.22}$$

Utilizing the next equalities,

$$\ln\left(\frac{\mathcal{S}(t-\xi_1)\mathcal{A}(t-\xi_1)}{\mathcal{S}\mathcal{A}}\right)=\ln\left(\frac{\mathcal{S}^*}{\mathcal{S}}\right)+\ln\left(\frac{S(t-\xi_1)\mathcal{A}(t-\xi_1)E^*}{\mathcal{S}^*\mathcal{A}^*\mathcal{E}}\right)+\ln\left(\frac{\mathcal{E}\mathcal{A}^*}{\mathcal{E}^*\mathcal{A}}\right),$$
$$\ln\left(\frac{\mathcal{E}(t-\xi_3)}{\mathcal{E}}\right)=\ln\left(\frac{\mathcal{A}\mathcal{E}^*}{\mathcal{E}\mathcal{A}^*}\right)+\ln\left(\frac{\mathcal{A}^*\mathcal{E}(t-\xi_3)}{\mathcal{A}\mathcal{E}^*}\right).$$

Equation (3.22) becomes

$$\frac{d\mathfrak{V}_2}{dt}=\Upsilon\Bigg[-(\gamma+m)\frac{(\mathcal{S}-\mathcal{S}^*)^2}{\mathcal{S}}-\beta_s\mathcal{S}^*\mathcal{A}^*\left(\frac{\mathcal{S}^*}{\mathcal{S}}-1-\ln\frac{\mathcal{S}^*}{\mathcal{S}}\right)$$
$$-\frac{e^{-m\xi_1}}{F}\beta_s\mathcal{S}^*\mathcal{A}^*\left(\frac{\mathcal{E}^*\mathcal{S}(t-\xi_1)\mathcal{A}(t-\xi_1)}{\mathcal{E}\mathcal{S}^*\mathcal{A}^*}-1-\ln\left(\frac{\mathcal{E}^*S(t-\xi_1)\mathcal{A}(t-\xi_1)}{\mathcal{E}\mathcal{S}^*\mathcal{A}^*}\right)\right)$$
$$-\frac{e^{-m\xi_3}}{G}\beta_s\mathcal{S}^*\mathcal{A}^*\left(\frac{\mathcal{A}^*\mathcal{E}(t-\xi_3)}{\mathcal{A}\mathcal{E}^*}-1-\ln\left(\frac{\mathcal{A}^*\mathcal{E}(t-\xi_3)}{\mathcal{A}\mathcal{E}^*}\right)\right)\Bigg]$$
$$=-\Upsilon(\gamma+m)\frac{(\mathcal{S}-\mathcal{S}^*)^2}{\mathcal{S}}-\Upsilon\beta_s\mathcal{S}^*\mathcal{A}^*Z\left(\frac{\mathcal{S}^*}{\mathcal{S}}\right)$$

$$- \frac{pGe^{-m\xi_1}}{(\omega+m)}\beta_s S^* \mathcal{A}^* Z\left(\frac{\mathcal{E}^* S(t-\xi_1)\mathcal{A}(t-\xi_1)}{\mathcal{E}\mathcal{S}^*\mathcal{A}^*}\right) - \frac{pFe^{-m\xi_3}}{(\omega+m)}\beta_s \mathcal{S}^* \mathcal{A}^* Z\left(\frac{\mathcal{A}^*\mathcal{E}(t-\xi_3)}{\mathcal{A}\mathcal{E}^*}\right).$$

It is easy to see that, if $\mathcal{S}^*, \mathcal{E}^*$, and $\mathcal{A}^* > 0$, then $\frac{d\mathfrak{W}_2}{dt} \leq 0$ for all $\mathcal{S}, \mathcal{E}$, and $\mathcal{A} > 0$. The solutions of the model (3.19) limit to Γ, the largest invariant subset of $\{\frac{d\mathfrak{W}_2}{dt} = 0\}$. It is observed that $\{\frac{d\mathfrak{W}_2}{dt} = 0\}$ if and only if $\mathcal{S} = \mathcal{S}^*$ and $Z = 0$, i.e.,

$$\frac{\mathcal{E}^*\mathcal{S}(t-\xi_1)\mathcal{A}(t-\xi_1)}{\mathcal{E}\mathcal{S}^*\mathcal{A}^*} = \frac{\mathcal{A}^*\mathcal{E}(t-\xi_3)}{\mathcal{A}\mathcal{E}^*} = 1. \tag{3.23}$$

If $\mathcal{S} = \mathcal{S}^*$, then from the first equation of (3.19) (when $\dot{\mathcal{S}}(t) = 0$), we have $\mathcal{A} = \mathcal{A}^*$, and from Eq (3.23), we get $\mathcal{E} = \mathcal{E}^*$. It follows that $\frac{d\mathfrak{W}_2}{dt}$ equals zero at D^*. LaSalle's invariance principle implies the global stability of D^*. □

Remark 1. *From the point of view of biology, $\kappa_v = 1$ means that the vaccine's efficacy is 100%, indicating that vaccinated cattle will remain uninfected by LSD. Theorem 3 suggests that the disease can still spread and reach a stable level, D^*, even if the vaccinated cattle are immune to the infection. The result indicates the need for additional strategies to control the spread of LSD (e.g., increasing the rate of vaccination [17], applying a quarantine strategy [23]). Numerical calculations confirm the identical outcome for $\kappa_v = 1$ (see Figure 6(a)) and for $\kappa_v \neq 1$ (see Figure 6(b)). Also, Figure 12 shows that although $\kappa_v = 1$, the result does not guarantee getting rid of the virus unless you use another method of delay. The analytic proof showing that the endemic point D^* of the whole model (2.1) is globally stable can be looked at in future research because it requires a new Lyapunov function.*

3.5. Sensitivity analysis

Sensitivity analysis is crucial for determining appropriate techniques to reduce virus transmission. Calculating sensitivity indices facilitates the examination of the influence of model parameters on R_0. This investigation outlines the most significant factors for mitigating disease development, offering essential insights for enhancing intervention strategies to manage lumpy skin disease (LSD).

We utilize the normalized forward sensitivity index, as outlined in [38] to assess the sensitivity of the parameters of the model. The sensitivity index for a specified parameter ζ is expressed as:

$$\Gamma_{\zeta}^{\mathsf{R}_0} = \frac{\partial \mathsf{R}_0}{\partial \zeta} \times \frac{\zeta}{\mathsf{R}_0}. \tag{3.24}$$

Thus, calculating all partial derivatives of the parameters with respect to R_0 and employing the formula (3.24) enables us to understand the impact of altering each parameter on R_0. For instance, a positive sensitivity index signifies that an increase in the relevant parameter results in an increase of the critical reproduction number, R_0, whereas a negative index implies that boosting the parameter diminishes R_0. Table 3 exhibits the parameters' effect on R_0, and for clarification, we display these values in the flowchart (see Figure 3). For example, the transmission rate β_s is directly proportional to R_0. The sensitivity index $\Gamma_{\beta}^{\mathsf{R}_0} = +0.80$ indicates that a 10% increase (or decrease) in the transmission rate β_s results in an 8% rise (or drop) in R_0. A higher interaction rate among cattle boosts the probability of infection. This aspect contributes to the establishment of an endemic system characterized by a high prevalence of lumpy skin disease. Consequently, diminishing β_s via

biosecurity protocols, including the management of insect vectors (e.g., mosquitoes and flies) and restricting cattle mobility, is crucial for decreasing the spread of diseases. Conversely, the vaccination rate γ possesses a sensitivity index of -0.40, indicating that a 10% increase in the vaccination rate will result in a 4.0% reduction in R_0. This emphasizes the efficacy of vaccination as a control measure against lumpy skin disease, as it reduces the susceptible cattle population and limits disease transmission. Similar to this, the delay of the LSD incubation period ξ_3 decreases R_0 by restricting the transmission of the virus prior to cattle being infectious. For example, administering the appropriate treatment to exposed cows can delay the appearance of symptoms and reduce the transmission of infection.

Additionally, to investigate how changes in various components impact the overall dynamics of the system, we plot the parameter changes against R_0 in Figure 4. Several factors influence R_0; these involve the proportion of cattle susceptible to LSD infection (λ), the transmission rate of LSD among susceptible cattle (β_s), the transmission rate of LSD among vaccinated cattle (β_v), the vaccination rate of susceptible cattle (γ), the incubation period for LSD (ξ_3), the mortality rate due to infection (σ), the delay in the transmission rate of infection (ξ_1), and the rate at which exposed cattle become infectious (p). A reduced effect with an absolute value (< 0.1) is noted for the transmission rate of vaccinated cattle (β_v) and the infection rate lag for vaccinated cattle (ξ_2). These findings match with the sensitivity analysis previously discussed. As a result, disease management techniques need to focus on factors with high sensitivity indices, since focused improvement may result in significant decreases in transmission. For instance, improving safety measures on cattle farms, performing fast and extensive vaccination plans, and limiting the movement of sick animals are essential management methods that can reduce the transmission rate of LSD across susceptible and vaccinated cattle with actively infected cattle. Furthermore, the incubation period for infected cattle can be extended with appropriate therapy to avoid subsequent infections. Furthermore, maintaining the health of livestock and preserving hygiene in areas visited by cattle, such as watering points and shelters, are essential measures in mitigating the transmission of lumpy skin disease.

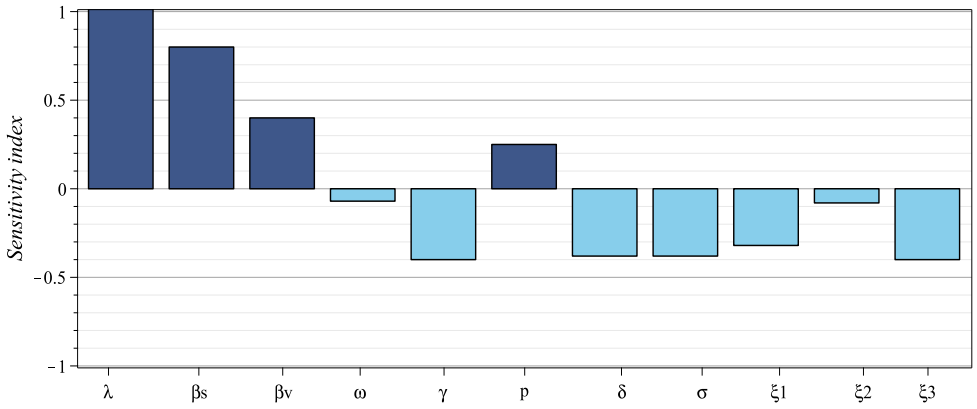

Figure 3. Sensitivity index of the parameters for model (2.1). The sensitivity index varies from -1 to $+1$. The highest index (in absolute value) shows the parameter to which the model output exhibits the greatest sensitivity: Here, it is λ followed by β_s, β_v, γ, ξ_3, δ, σ, ξ_1, and p. The index of each of the other parameters is below 0.1.

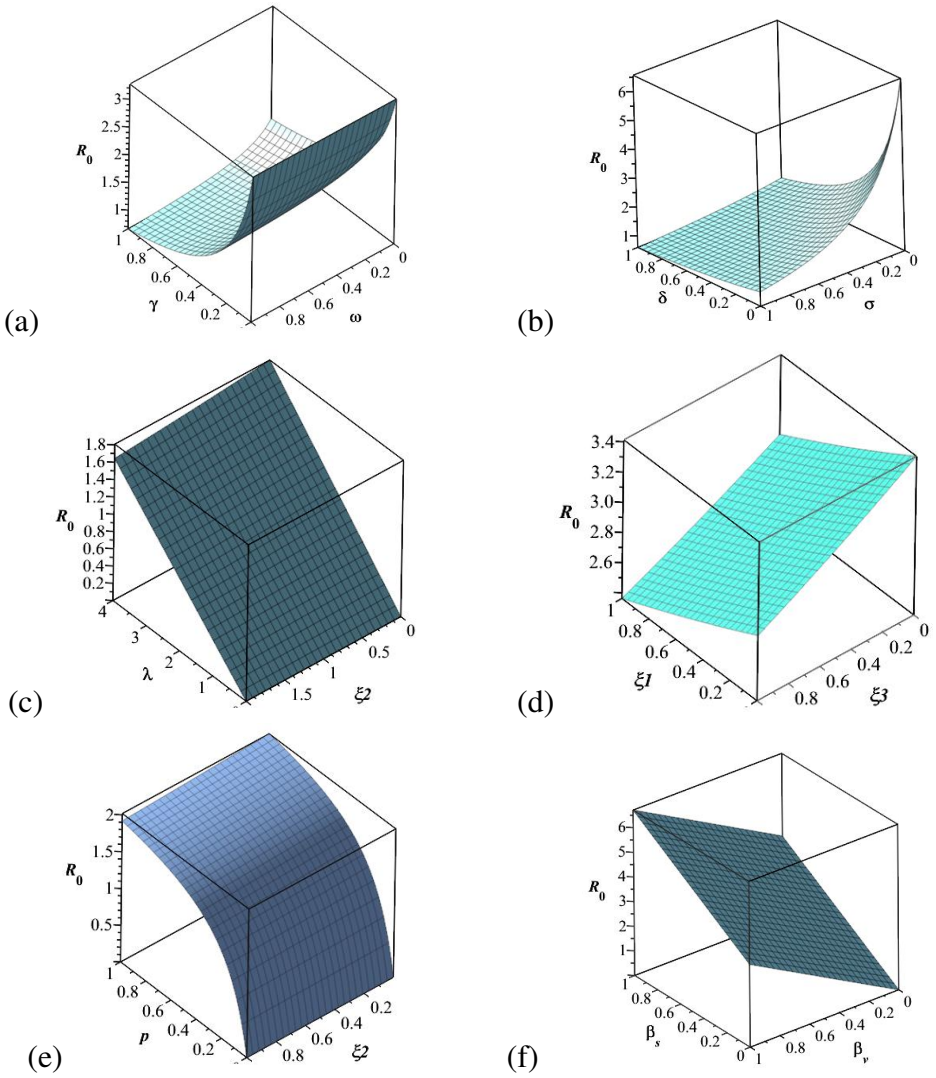

Figure 4. The impact of changing model parameters on R_0: (a) $\mathcal{R}_0$ v.s. γ and ω; (b) R_0 v.s. δ and σ; (c) R_0 v.s. λ and ξ_2; (d) R_0 v.s. ξ_1 and ξ_3; (e) R_0 v.s. p and ξ_2; (f) R_0 v.s. β_s and β_v.

Table 3. Sensitivity index of the model parameters (2.1). The parameter values are at baseline as detailed in Table 2.

Parameter	λ	β_s	β_v	ω	γ	p	δ	σ	ξ_1	ξ_2	ξ_3
Sensitivity index	1	0.80	0.40	-0.07	-0.40	0.25	-0.38	-0.38	-0.32	-0.08	-0.40

4. Numerical simulation

A numerical approach for the delayed lumpy skin disease model (2.1) has been established. We conduct all calculations using MATLAB's built-in solver dde23, which is specifically designed for delay differential equations. The solver is based on the Bogacki–Shampine Runge–Kutta method and employs adaptive step-size control to ensure accuracy. First, we show the dynamical behavior of model (2.1) as the solutions approach the two different equilibriums discussed in Section 3.2 (see

Figures 5 and 6). Here we will use the baseline parameters listed in Table 1. Without losing generality, we set $\xi_e = \xi_1 = \xi_2 = \xi_3$. The parameter ξ_e shall be selected below.

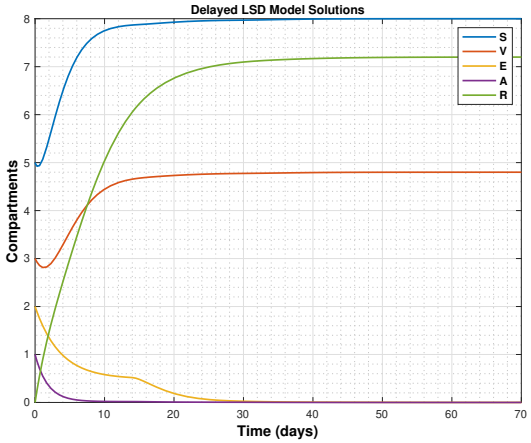

Figure 5. Solutions of model (2.1), taking into consideration the values of the baseline parameters presented in Table 2, where $\xi_e = \xi_1 = \xi_2 = \xi_3 = 14$ and $\mathcal{R}_0 = 0.01 < 1$. Then D^0 is GAS.

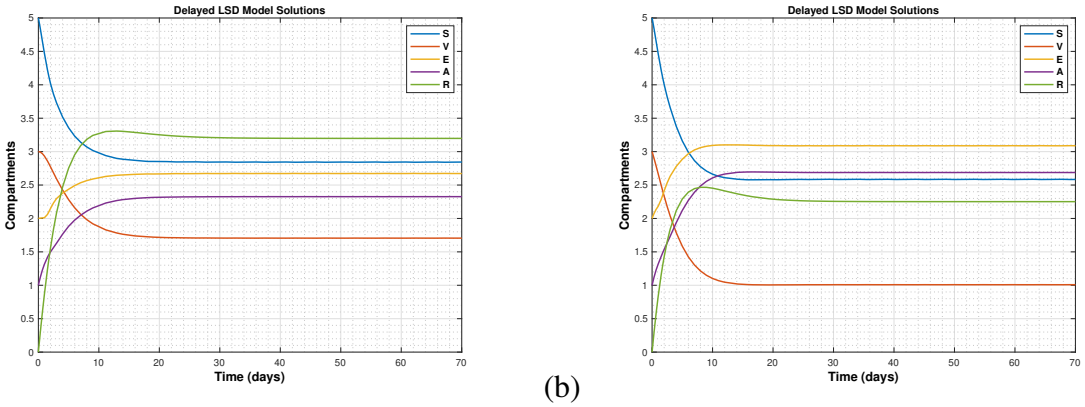

(a) (b)

Figure 6. Solutions of model (2.1), when $p = 0.59$, $\xi_e = \xi_1 = \xi_2 = \xi_3 = 1$, and $\mathcal{R}_0 > 1$ in two different aspects: (a) $\kappa_v = 1$ (i.e., the efficacy of the vaccine is 100%), and then $\mathcal{R}_0 = 2.81 > 1$; (b) $\kappa_v = 0.5$, and therefore, $\mathcal{R}_0 = 3.25 > 1$ and D^* is GAS.

(A) $\mathsf{R}_0 \leq 1$. Choose $\xi_e = 14$ and we obtain $\mathsf{R}_0 = 0.01$. In accordance with Theorem 2, D^0 is GAS. Figure 5 shows that the numerical and theoretical results in Theorem 2 are equivalent. The susceptible, vaccinated, and recovering LSD cattle are rising and approaching their respective values. The corresponding values are

$$\mathcal{S}_0 = \frac{\lambda}{\gamma + m} \approx 8,\ \mathcal{V}_0 = \frac{\lambda\gamma}{(\omega + m)(\gamma + m)} \approx 4.79,\ \textit{and}\ \mathsf{R}_0 = \frac{\lambda\omega\gamma}{m(\omega + m)(\gamma + m)} \approx 7.20.$$

The number of individuals in exposed and active LSD compartments is decreasing and exceeding zero.
(B) $\mathsf{R}_0 > 1$. Choose $\xi_e = 1$, and we have two different cases. (a) $\kappa_v = 1$, and then we get $\mathsf{R}_0 = 2.81$, and

(b) $\kappa_v = 0.5 \neq 1$, and we get $\mathsf{R}_0 = 3.25$. Figure 6 demonstrates that the numerical findings agree with the theoretical conclusions of Theorem 3, where D^* is GAS. The solutions of model (2.1) approach (a) $D^* = (2.8, 1.71, 2.67, 2.33, 3.20)$, where $\kappa_v = 1$, and (b) $D^* = (2.59, 1, 3.08, 2.69, 2.25)$, where $\kappa_v = 0.5 \neq 1$.

We will now investigate the methods by which the epidemic can be effectively controlled. One of the principal strategies for disease control is to make successful use of delays. Therefore, in the initial scenario, we examine the impact of varying delay levels on the dynamics of the LSD. Second, we examine the role of efficacy κ_v in disease control. Finally, the role of vaccine effectiveness and time delays on the basic reproductive number will be studied.

4.1. Impact of the time delays on the dynamics of the model

In the first case, we are going to fix the LSD vaccine efficacy, $\kappa_v = 0.5$. Figures 7 and 8 demonstrate the impact of lag parameters on the progression of exposed and active LSD cattle. In Figures 7(a) and (b), when increasing ξ_1 from 3 to 14, one can see that a gradual decline in exposed and active LSD individuals approaches zero. This indicates that the LSD outbreak is being effectively managed. However, in sub-panels (c) and (d), a longer ξ_2 slightly reduces the levels of exposed and active LSD individuals in the long term, but it will not eradicate the infection. Figures 8(a) and (b) show that increasing the delay of exposed cattle from becoming active with LSD from ($\xi_3 = 3$) to ($\xi_3 = 6$) tends to reduce the number of active and exposed LSD cattle. When $\xi_3 = 10$, we can see that both populations are vanishing. Furthermore, sub-panels (c) and (d) show that when we increase the common delay ξ_e, an earlier time of delay ($\xi_e = 6$ days) leads to eliminating both exposed and active compartments compared with the previous cases (i.e., increasing ξ_i, $i = 1, 2, 3$) separately. This indicates the importance of using a combination of delay strategies to reduce LSD infection rather than using one strategy, for example, increasing ξ_1, the period of LSD transmission between those who are susceptible to infection and the active LSD cattle, through physical isolation or vaccination as well as increasing ξ_3, the period of incubation for the exposed cattle, by providing them medication to delay the LSD virus from becoming infectious.

Figures 9 and 10 show the role of time delays on the number of $\mathcal{S}$, $\mathcal{V}$, and $\mathcal{R}$ over time. Figure 9 clearly analyzes the effects of delays in infection exposure (ξ_1, ξ_2), whereas Figure 10 explores the consequences of symptom onset (ξ_3) and a common delay parameter (ξ_e). In Figure 9(a), extending ξ_1 (from 3 to 14 days) markedly modifies the system dynamics. Longer delays lead to an increased number of susceptible, vaccinated, and recovered individuals at equilibrium. The transient dynamics exhibit increasingly significant oscillations with increased delays; however, stability occurs over time. Figure 9(b) shows that increasing ξ_2 has minor influence on long-term dynamics. $\mathcal{S}$, $\mathcal{V}$, and $\mathcal{R}$ quickly converge to a stable state with minimal change across different choices of ξ_2. The system stabilizes more rapidly than with changes in ξ_1, indicating that ξ_2 has a lower impact on changing disease dynamics. This suggests that the vaccinated population exhibits relative stability against exposure delays, indicating that vaccine-induced protection decreases sensitivity to infection timing. Figures 10(a) and (b) present that both ξ_3 and ξ_e significantly influence the epidemic trajectory, with long lags resulting in increased equilibrium values throughout all states. The common delay parameter (ξ_e) has a more significant impact than the symptom onset delay (ξ_3).

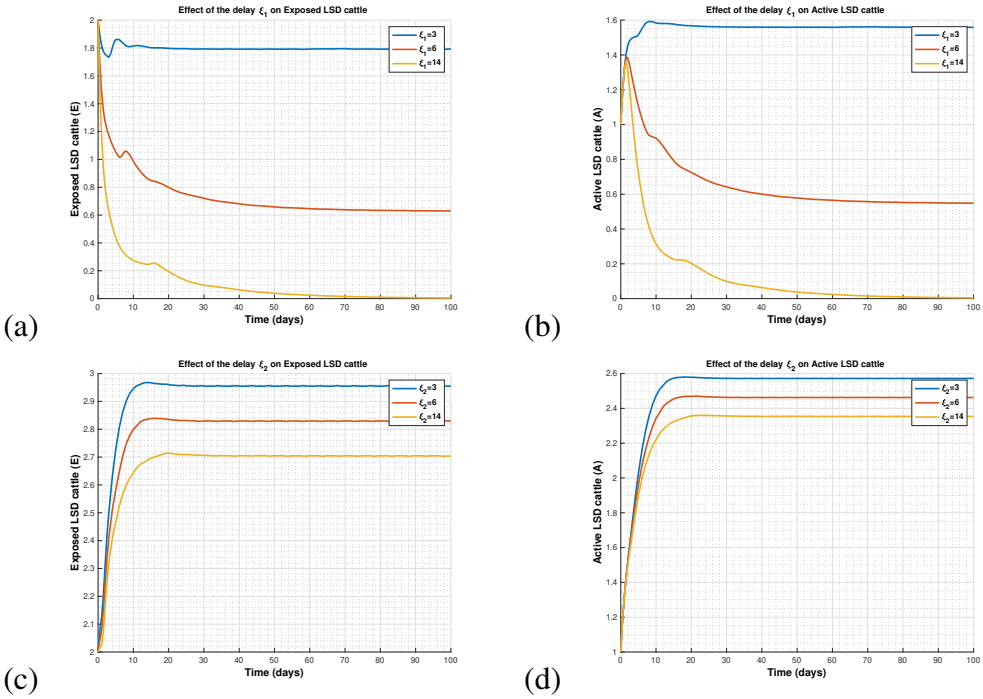

Figure 7. Graphic representation of the dynamics: (a), (c) exposed, and (b), (d) active LSD cattle of model (2.1), as we vary the delays: (a)-(b) time delay for the LSD transmission of the susceptible cattle, ξ_1; and (c)-(d) time delay for the LSD transmission of the vaccinated cattle, ξ_2.

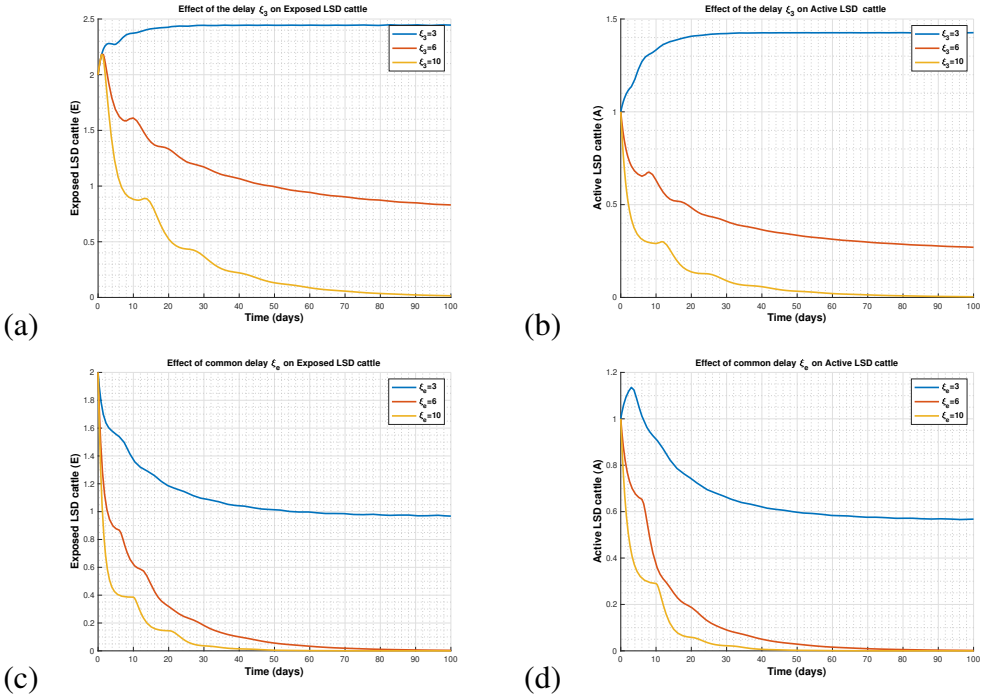

Figure 8. Graphic representation of the dynamics: (a), (c) exposed, and (b), (d) active LSD cattle of model (2.1), as we vary the delays: (a)-(b) time delay for the exposed cattle to be active (infectious), ξ_3; and (c)-(d) common time delay, ξ_e, for model (2.1).

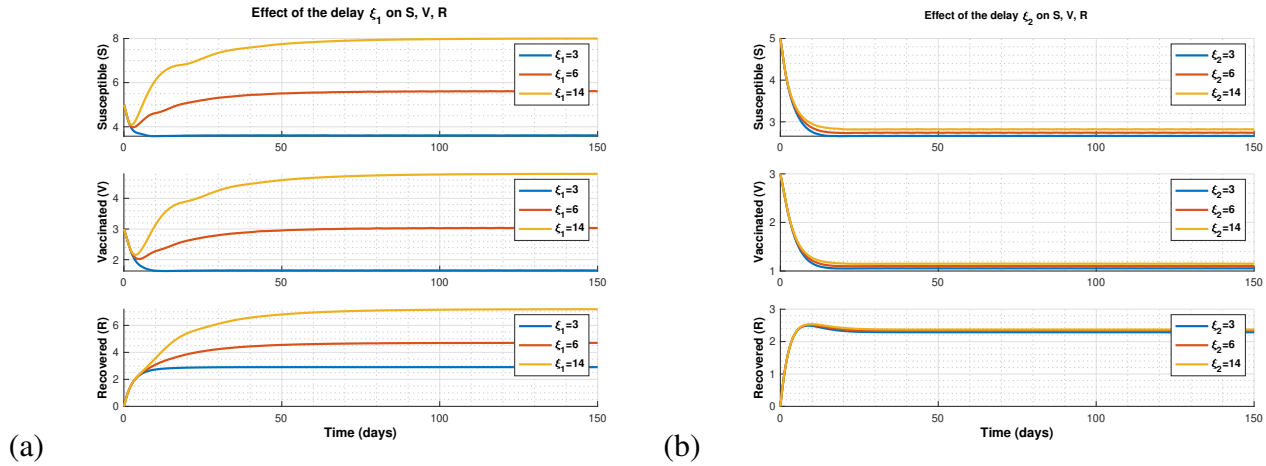

(a) (b)

Figure 9. Graphic representation of the dynamics: susceptible, vaccinated, and recovered LSD cattle of model (2.1), as we vary (a) the delay in the exposure to infection for $\mathcal{S}$, ξ_1; and (b) the delay in the exposure to infection for $\mathcal{V}$, ξ_2.

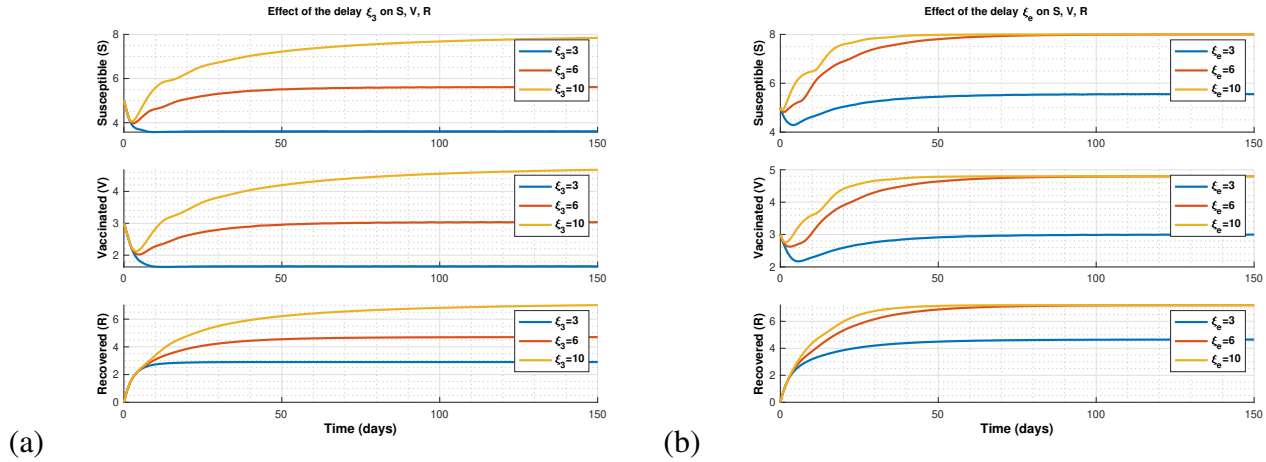

(a) (b)

Figure 10. Graphic representation of the dynamics: susceptible, vaccinated, and recovered LSD cattle of model (2.1), as we vary (a) the delay in the onset of LSD symptoms following an infection, ξ_3; and (b) the common delay, ξ_e.

4.2. Impact of vaccine efficacy on the dynamics of the model

Figure 11 shows that increasing vaccination efficacy ($\kappa_v = 1.0$) shifts the cattle population towards vaccinated and recovered classes, while decreasing the numbers of susceptible, exposed, and active cases. Partial vaccination efficacy ($\kappa_v = 0.5$) offers moderate control, lowering infection rates compared to no vaccination; however, it is less efficient than full vaccination. The lack of vaccination efficacy ($\kappa_v = 0.0$) results in a raised infection prevalence associated with an increased number of exposed and active cases, although recovery remains restricted. This analysis highlights the essential importance of immunization in managing LSD outbreaks. Increasing vaccination rates decreases disease transmission, reduces active and exposed cases, and supports herd immunity by boosting the recovered population. However, it does not eradicate the infection from the cattle herd. Consequently,

relying solely on effective vaccines without implementing supplementary techniques–such as increasing the rate of vaccinated cattle [17], enforcing biosecurity measures, and controlling vectors–may not be sufficient to eliminate the virus from the population.

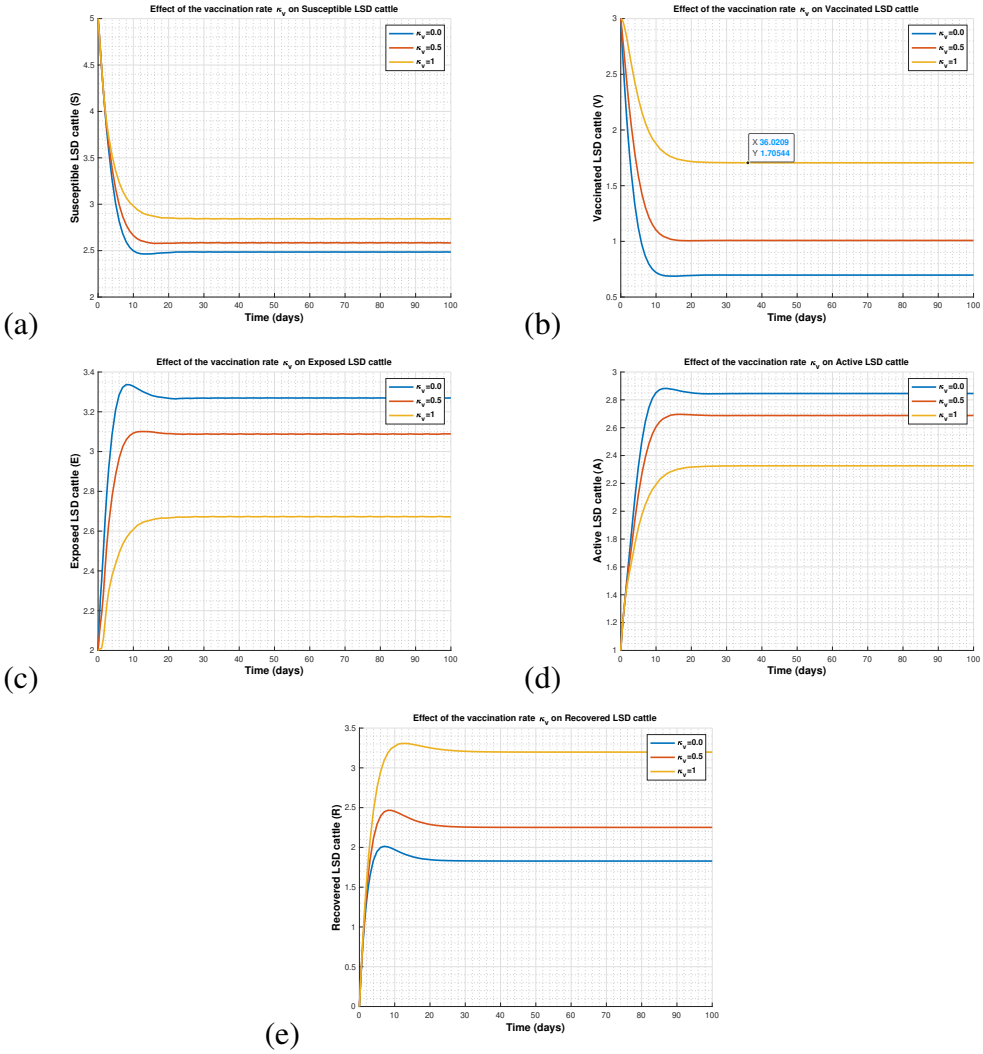

Figure 11. Graphic representation of the dynamics of model (2.1), as we vary the vaccine efficacy (κ_v), where $\xi_1 = \xi_2 = \xi_3 = 1$. Sub-panels (a) susceptible LSD cattle, $\mathcal{S}$; (b) vaccinated LSD cattle, $\mathcal{V}$; (c) exposed LSD cattle, $\mathcal{E}$; (d) active LSD cattle, $\mathcal{A}$; (e) recovered LSD cattle, $\mathcal{R}$.

4.3. Impact of the vaccine efficacy and the time delays on the basic reproduction number

Figure 12 illustrates the influence of varying the parameters κ_v, ξ_i $(i = 1, 2, 3)$ on the reproduction number R_0. We observe that, in sub-figures (a,c,d), as the vaccine efficacy or the time delays increase, R_0 decreases until it becomes less than one, and then the given model switches from endemic equilibrium to free LSD equilibrium. Therefore, the absence of LSD is stable. However, sub-figure (b) shows that the delay, ξ_2, has a smaller effect on R_0; this means that increasing the time delay between vaccinated and active LSD cattle can help slow down the spread of LSD infection but will

not completely get rid of the virus in the population. Sub-figure (d) shows that LSD spread can be controlled in a shorter period compared to the previous cases. We can see that increasing the common delay ξ_e while increasing κ_v leads to faster elimination of the virus. Let $\kappa_v = 1$; we can see that when $\xi_e \approx 3.8$ days, R_0 becomes less than 1, while in the same value of κ_v, we need more time delay (e.g., $\xi_1 = \xi_3 \approx 6$ days) to stabilize the solutions around the LSD-free equilibrium (i.e., $\mathsf{R}_0 < 1$). Therefore, using several strategies of control, e.g., vaccinations, isolation, and treatment, can reduce the disease more effectively. From a biological perspective, the delay works equivalently to antiviral medication and vaccines in reducing the LSD outbreak. We observe that, even in the absence of vaccine efficacy (i.e., $\kappa_v = 0$), a sufficiently long delay inhibits viral spread and eliminates the LSD virus (see sub-figures (c) and (d)). This offers novel ideas for medication development using delay strategies, including vaccination, quarantine, drugs, limitations on travel holidays, and distancing measures, which have a crucial role in controlling the present strain of the LSD virus by extending the intracellular delay period. From sub-figures (a), (c), and (d), we can see that even with the efficacy of vaccine $\kappa_v = 1$, this cannot eliminate the LSD virus, unless we extend one or more intracellular time delays, i.e., increase ξ_1 or ξ_3, or increase the common delay ξ_e. This supports our results in Figure 11.

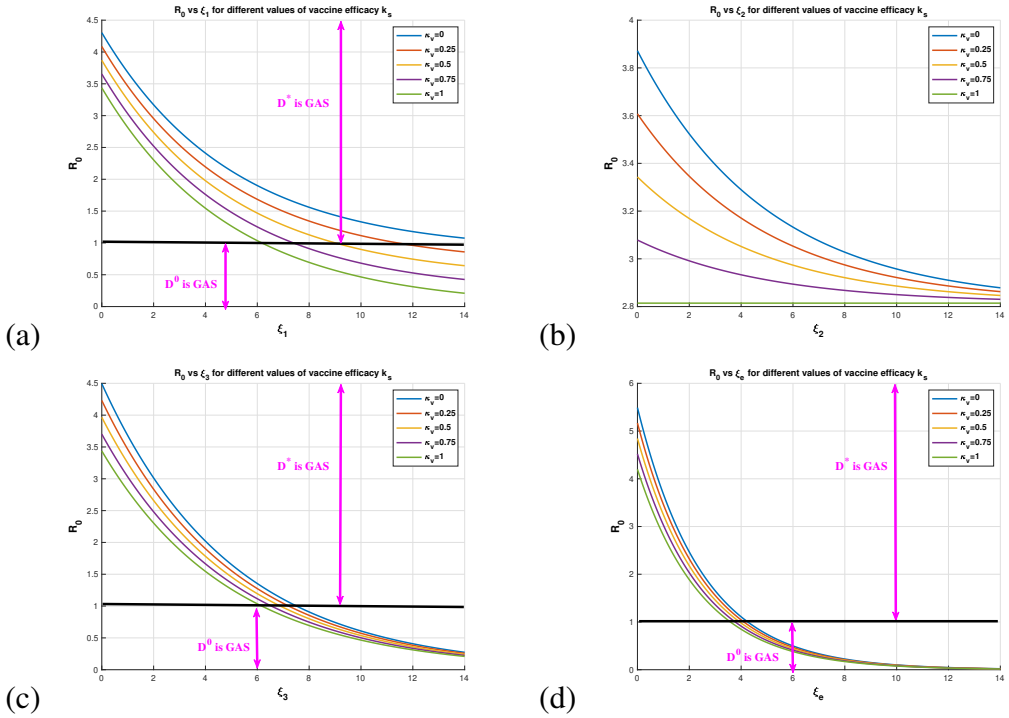

Figure 12. Effects of the vaccine efficacy and the time delays on the reproduction number for model (2.1): (a) Effect of ξ_1 on R_0, where $\xi_2 = \xi_3 = 1$; (b) Effect of ξ_2 on R_0, where $\xi_1 = \xi_3 = 1$; (c) Effect of ξ_3 on R_0, where $\xi_1 = \xi_2 = 1$; (d) Effect of ξ_e on R_0, where $\xi_e = \xi_1 = \xi_2 = \xi_3$.

5. Conclusions

This work investigated the lumpy skin disease model, incorporating vaccine efficacy and different types of time delays to control the spread of LSD. Initially, we conducted a theoretical analysis of the

model by demonstrating its biologically significant aspects. We proved that the model exhibits both local and global stability at equilibrium places. The basic reproduction ratio R_0, which establishes the global dynamics of the delayed-LSD model, has been investigated. We have shown that the LSD-free equilibrium point is GAS when $R_0 \leq 1$, and the LSD-endemic equilibrium is GAS when $R_0 > 1$. We completed a sensitivity analysis to assess the impact of model parameters on the reproduction number R_0 and identified the most critical parameters. Next, we explored the impact of the vaccine's efficacy and different types of delays on the spread of LSD. From a biological perspective, the delays act similarly to antiviral vaccines and medications in suppressing the LSD outbreak. The results showed that applying a combination of delays is more effective in eliminating the LSD virus outbreak. Furthermore, it is observed that, even without an effective vaccination, an extended period of time effectively limits viral transmission and prevents the LSD virus. Applying a single delay strategy necessitates more time to eradicate the LSD disease. Moreover, the findings highlight that even with a vaccination indicating 100% efficacy with a specific vaccination rate of 30% for susceptible cattle, the eradication of the disease from populations is unlikely until additional mitigation methods are implemented. Some examples of applying delay strategies are integrating vaccination, quarantine, treatment, and restriction of movements to control the disease's spread (for more details, see [39, 40]). These approaches, which are based on model sensitivity analysis and simulations, provide stakeholders, including agriculturalists, veterinarians, and officials, with the necessary data to manage LSD successfully.

This work has some drawbacks: First: Our model assumes that recovered or vaccinated cattle maintain protective immunity throughout the study period; however, immunity to the LSD virus may be waning or variable, which could impact the estimated basic reproduction number (R_0) and the thresholds for disease eradication [41]. Second: Vector-borne routes significantly influence the movement of LSD, primarily through biting flies and mosquitoes. The specific dynamics of these vectors, such as seasonal abundance, climate variability, and control interventions, were not precisely specified in this analysis. Changes in vector populations may significantly impact transmission dynamics, epidemic size, and the effectiveness of control strategies [42–44]). Third: In our model, we ignore a spatially dependent reaction–diffusion framework that incorporates diffusion coefficients of cattle and vector, and then perform stability analysis to determine outbreak and control conditions [45]. Finally, combining vaccination and delay with contact restrictions may serve as an effective control strategy for lumpy skin disease. Time delays in the model could reflect behavioral or policy-driven interventions, including decreased interactions between susceptible and infectious cattle resulting from quarantine, movement limitations, or voluntary biosecurity measures. In accordance with the methodology in [46], contact restrictions can be implemented by reducing the effective transmission rate over time; for instance, in our model, we can replace $\beta_s = (1 - u_s(t))\beta_{s1}$, where $u_s(t)$ $(0 \leq u_s(t) \leq 1)$ denotes the intensity of the constraint. These methods are expected to reduce the infection peak and postpone the growth of the outbreak, hence improving the efficacy of vaccination and other control strategies.

Use of Generative-AI tools declaration

The author declares she has not used Artificial Intelligence (AI) tools in the creation of this article.

Acknowledgments

The author is grateful to the unknown referees for the many constructive suggestions, which helped to improve the presentation of the paper.

Conflict of interest

The author declares no conflict of interest.

References

1. A. Kononov, P. Prutnikov, I. Shumilova, S. Kononova, A. Nesterov, O. Byadovskaya, et al., Determination of lumpy skin disease virus in bovine meat and offal products following experimental infection, *Transbound. Emerg. Dis.*, **66** (2019), 1332–1340. https://doi.org/10.1111/tbed.13158
2. E. Mulatu, A. Feyisa, Review: Lumpy skin disease, *J. Vet. Sci. Technol.*, **9** (2018), 535. https://doi.org/10.4172/2157-7579.1000535
3. X. Roche, A. Rozstalnyy, D. TagoPacheco, C. Pittiglio, A. Kamata, D. B. Alcrudo, et al., *Introduction and spread of lumpy skin disease in South, East and Southeast Asia: Qualitative risk assessment and management*, Rome: Food and Agriculture Organization of the United Nations, 2021.
4. B. Datten, A. A. Chaudhary, S. Sharma, L. Singh, K. D. Rawat, M. S. Ashraf, et al., An extensive examination of the warning signs, symptoms, diagnosis, available therapies, and prognosis for lumpy skin disease, *Viruses*, **15** (2023), 604. https://doi.org/10.3390/v15030604
5. S. A. Alharbi, N. A. Almuallem, Computational study of a fractional-order HIV epidemic mdel with latent phase and treatment, *Fractal Fract.*, **9** (2025), 28. https://doi.org/10.3390/fractalfract9010028
6. N. A. Almuallem, H. M. Ali, E. M. Elsaid, M. R. Eid, W. S. Hassanin, Mathematical simulation of optimal control measures to avoid chickenpox infection, *Int. J. Math. Math. Sci.*, **2025** (2025), 3238188. https://doi.org/10.1155/ijmm/3238188
7. A. I. Butt, W. Ahmad, M. Rafiq, D. Baleanu, Numerical analysis of Atangana-Baleanu fractional model to understand the propagation of a novel corona virus pandemic, *Alex. Eng. J.*, **61** (2022), 7007–7027. https://doi.org/10.1016/j.aej.2021.12.042
8. N. A. Almuallem, H. Mollah, S. Sarwardi, A study of a prey-predator model with disease in predator including gestation delay, treatment and linear harvesting of predator species, *AIMS Math.*, **10** (2025), 14657–14698. https://doi.org/10.3934/math.2025660
9. P. O. Odeniran, A. A. Onifade, E. T. MacLeod, I. O. Ademola, S. Alderton, S. C. Welburn, Mathematical modelling and control of African animal trypanosomosis with interacting populations in West Africa-Could biting flies be important in main taining the disease endemicity? *PLoS One*, **15** (2020), e0242435. https://doi.org/10.1371/journal.pone.0242435

10. R. Bradhurst, G. Garner, M. Hóvári, M. de la Puente, K. Mintiens, S. Yadav, et al., Development of a transboundary model of livestock disease in Europe, *Transbound. Emerg. Dis.*, **69** (2022), 1963–1982. https://doi.org/10.1111/tbed.14201

11. E. L. Brugnago, E. C. Gabrick, K. C. Iarosz, J. D. Szezech, R. L. Viana, A. M. Batista, et al., Multistability and chaos in SEIRS epidemic model with a periodic time-dependent transmission rate, *Chaos*, **33** (2023), 123123. https://doi.org/10.1063/5.0156452

12. E. C. Gabrick, E. L. Brugnago, S. L. de Souza, K. C. Iarosz, J. D. Szezech, R. L. Viana, et al., Impact of periodic vaccination in SEIRS seasonal model, *Chaos*, **34** (2024), 013137. https://doi.org/10.1063/5.0169834

13. A. C. Costa, D. L. Cardoso, L. F. de Oliveira, I. R. de Oliveira, S. Bhowmick, M. Amaku, et al., Network analysis of cattle movement among municipalities in Minas Gerais State, Brazil, from 2013 to 2023, *Prevent. Vet. Med.*, **236** (2025), 106420. https://doi.org/10.1016/j.prevetmed.2025.106420

14. I. A. Moneim, D. Greenhalgh, Threshold and stability results for an SIRS epidemic model with a general periodic vaccination strategy, *J. Biol. Syst.*, **13** (2005), 131–150. https://doi.org/10.1142/S0218339005001446

15. R. Magori-Cohen, Y. Louzoun, Y. Herziger, E. Oron, A. Arazi, E. Tuppurainen, et al., Mathematical modelling and evaluation of the different routes of transmission of lumpy skin disease virus, *Vet. Res.*, **43** (2012), 1. https://doi.org/10.1186/1297-9716-43-1

16. A. Anwar, K. Na-Lampang, N. Preyavichyapugdee, V. Punyapornwithaya, Lumpy skin disease outbreaks in Africa, Europe, and Asia (2005–2022): multiple change point analysis and time series forecast, *Viruses*, **14** (2022), 2203. https://doi.org/10.3390/v14102203

17. A. I. Butt, H. Aftab, M. Imran, T. Ismaeel, Mathematical study of lumpy skin disease with optimal control analysis through vaccination, *Alex. Eng. J.*, **72** (2023), 247–259. https://doi.org/10.1016/j.aej.2023.03.073

18. G. Man, A. J. Gnanaprakasam, S. Ramalingam, A. S. Omer, I. Khan, Mathematical model of the lumpy skin disease using Caputo fractional-order derivative via invariant point technique, *Sci. Rep.*, **15** (2025), 9112. https://doi.org/10.1038/s41598-025-92884-y

19. G. Saha, P. Shahrear, A. Faiyaz, A. K. Saha, Mathematical modeling of lumpy skin disease: New perspectives and insights, *PDE Appl. Math.*, **30** (2025), 101218.

20. W. F. Alfwzan, M. H. DarAssi, F. M. Allehiany, M. A. Khan, M. Y. Alshahrani, E. M. Tag-Eldin, A novel mathematical study to understand the Lumpy skin disease (LSD) using modified parameterized approach, *Results Phys.*, **51** (2023), 106626. https://doi.org/10.1016/j.rinp.2023.106626

21. G. Gari, A. Waret-Szkuta, V. Grosbois, P. Jacquiet, F. Roger, Risk factors associated with observed clinical lumpy skin disease in Ethiopia, *Epidemiol. Inf.*, **138** (2010), 1657–1666. https://doi.org/10.1017/S0950268810000506

22. P. Kumar, S. Kumar, B. S. Alkahtani, S. S. Alzaid, A robust numerical study on modified Lumpy skin disease model, *AIMS Math.*, **9** (2025), 22941–22985. https://doi.org/10.3934/math.20241116

23. N. A. Almuallem, R. P. Chauhan, Effects of quarantine and vaccination on the transmission of Lumpy skin disease: A fractional approach, *PLoS One*, **20** (2025), e0327673. https://doi.org/10.1371/journal.pone.0327673

24. S. A. Ambhore, N. K. Lamba, Lumpy skin disease: A mathematical model application, *Indian J. Sci. Technol.*, **18** (2025), 755–762.

25. A. M. Elaiw, N. A. Almuallem, Global properties of delayed-HIV dynamics models with differential drug efficacy in cocirculating target cells, *Appl. Math. Comput.*, **15** (2015), 1067–1089. https://doi.org/10.1016/j.amc.2015.06.011

26. M. H. Hassan, T. El-Azab, G. AlNemer, M. A. Sohaly, H. El-Metwally, Analysis time-delayed SEIR model with survival rate for COVID-19 stability and disease control, *Mathematics*, **12** (2024), 3697. https://doi.org/10.3390/math12233697

27. E. Tuppurainen, K. Dietze, J. Wolff, H. Bergmann, D. Beltran-Alcrudo, A. Fahrion, et al., Review: Vaccines and vaccination against lumpy skin disease, *Vaccines*, **9** (2021), 1136. https://doi.org/10.3390/vaccines9101136

28. M. M. Ojo, O. J. Peter, E. F. Goufo, H. S. Panigoro, F. A. Oguntolu, Mathematical model for control of tuberculosis epidemiology, *J. Appl. Math. Comput.*, **69** (2023), 69–87.

29. Y. Kuang, *Delay differential equations: with applications in population dynamics*, New York: Academic press, 1993.

30. Y. Narwal, S. Rathee, Fractional order mathematical modeling of lumpy skin disease, *Commun. Faculty Sci. Uni. Ankara Ser. A1 Math. Stat.*, **73** (2024), 192–210. https://doi.org/10.31801/cfsuasmas.1207144

31. A. El-Mesady, A. A. Elsadany, A. M. Mahdy, A. Elsonbaty, Nonlinear dynamics and optimal control strategies of a novel fractional-order lumpy skin disease model, *J. Comput. Sci.*, **79** (2024), 102286. https://doi.org/10.1016/j.jocs.2024.102286

32. O. Arino, M. L. Hbid, E. Ait Dads, Delay differential equations and applications, In: *Proceedings of the NATO Advanced Study Institute held in Marrakech, Morocco, 9-21 September 2002*, Springer Science & Business Media, 2007.

33. X. Yang, L. Chen, J. Chen, Permanence and positive periodic solution for the single-species nonautonomous delay diffusive models, *Comput. Math. Appl.*, **32** (1996), 109–116.

34. P. Van den Driessche, J. Watmough, Reproduction numbers and sub-threshold endemic equilibria for compartmental models of disease transmission, *Math. Biosci.*, **180** (2002), 29–48. https://doi.org/10.1016/S0025-5564(02)00108-6

35. N. Chitnis, J. M. Cushing, J. M. Hyman, Bifurcation analysis of a mathematical model for malaria transmission, *SIAM J. Appl. Math.*, **67** (2006), 24–45. https://doi.org/10.1137/050638941

36. J. K. Hale, S. M. Lunel, *Introduction to functional differential equations*, Berlin: Springer Science & Business Media, 2013.

37. J. P. La Salle, *The stability of dynamical systems*, USA: Society for Industrial and Applied Mathematics, 1976.

38. N. Chitnis, J. M. Hyman, J. M. Cushing, Determining important parameters in the spread of malaria through the sensitivity analysis of a mathematical model, *Bull. Math. Biol.*, **70** (2008), 1272–1296. https://doi.org/10.1007/s11538-008-9299-0

39. F. Namazi, A. Khodakaram Tafti, Lumpy skin disease, an emerging transboundary viral disease: A review, *Vet. Med. Sci.*, **7** (2021), 888–896. https://doi.org/10.1002/vms3.434 .

40. P. M. Beard, Lumpy skin disease: A direct threat to Europe, *Vet. Rec.*, **178** (2016), 557–558. https://doi.org/10.1136/vr.i2800

41. M. T. Al-Arydah, Assessing vaccine efficacy for infectious diseases with variable immunity using a mathematical model, *Sci. Rep.*, **14** (2024), 18572. https://doi.org/10.1038/s41598-024-69651-6

42. M. T. Al-Arydah, R. Smith, Controlling malaria with indoor residual spraying in spatially heterogenous environments, *Math. Biosci. Eng.*, **8** (2011), 889–914. https://doi.org/10.3934/mbe.2011.8.889

43. A. I. Butt, Dynamical modeling of lumpy skin disease using Atangana-Baleanu derivative and optimal control analysis, *Model. Earth Syst. Environ.*, **11** (2025), 27. https://doi.org/10.1007/s40808-024-02239-1

44. A. I. Butt, H. Aftab, M. Imran, T. Ismaeel, M. Arab, M. Gohar, et al., Dynamical study of lumpy skin disease model with optimal control analysis through pharmaceutical and non-pharmaceutical controls, *Europ. Phys. J. Plus*, **138** (2023), 1048. https://doi.org/10.1140/epjp/s13360-023-04690-y

45. V. Osei-Buabeng, A. A. Frimpong, B. Barnes, Mathematical modeling of COVID-19 with a constant spatial diffusion term in Ghana, *Comput. Meth. Diff. Equ.*, **13** (2025), 870–884. https://doi.org/10.22034/cmde.2024.59036.2504

46. S. L. de Souza, A. M. Batista, I. L. Caldas, K. C. Iarosz, J. D. Szezech, Dynamics of epidemics: Impact of easing restrictions and control of infection spread, *Chaos Solitons Fract.*, **142** (2021), 110431. https://doi.org/10.1016/j.chaos.2020.110431

AIMS Press